Precambrian Research 255 (2014) 276–293

Contents lists available at ScienceDirect

Precambrian Research

journal homepage: www.elsevier.com/locate/precamres

Paleo-position of the North China craton within the supercontinent Columbia: Constraints from new paleomagnetic results

Huiru Xu[a,b,*], Zhenyu Yang[c,d], Peng Peng[a], Joseph G. Meert[e], Rixiang Zhu[a]

[a] State Key Laboratory of Lithospheric Evolution, Institute of Geology and Geophysics, Chinese Academy of Science, Beijing 100029, China
[b] University of Chinese Academy of Sciences, Beijing 100049, China
[c] Key Laboratory of Paleomagnetism and Tectonic Reconstruction, Ministry of Land and Resource, Beijing 100081, China
[d] Institute of Geomechanics, Chinese Academy of Geological Sciences, Beijing 100081, China
[e] Department of Geological Sciences, University of Florida, Gainesville, FL 32611, USA

ARTICLE INFO

Article history:
Received 22 February 2014
Received in revised form
30 September 2014
Accepted 3 October 2014
Available online 14 October 2014

Keywords:
North China craton
Mafic dyke swarm
Xiong'er volcanic rocks
Paleomagnetism
Columbia
Supercontinent

ABSTRACT

Several new paleomagnetic and geological studies focused on the reconstruction of the North China Craton (NCC) within the Paleo-Mesoproterozoic Columbia supercontinent. In spite of these new data, there are still widely divergent opinions regarding supercontinental reconstructions. In addition to qualitative correlations of orogenic belts, rift basin ages, stratigraphy and distribution of igneous provinces, paleomagnetic data can provide key constraints on the positioning of individual cratons on the globe. In this paper, we report a detailed paleomagnetic study on the coeval ~1780 Ma mafic dyke swarm and Xiong'er volcanic province, which extended for more than one thousand kilometers in the central NCC. Rock magnetic studies, including thermomagnetic curves, hysteresis loops and the progressive acquisition of isothermal remanence conducted in selected samples, indicate that the dominant magnetic carriers are PSD magnetite. Stepwise thermal demagnetization isolated higher-temperature components directed to NNE/SSW with shallow inclinations from 37 sampling sites (16 sites in Yinshan area, 13 sites in Taihang area and 8 sites in Xiaoshan area). A baked contact test conducted on two Yinshan dykes intruded by a younger dyke demonstrates the magnetization in the Yinshan dykes pre-dates 1320 Ma. The existence of dual-polarity magnetizations in both Taihang and Xiong'er areas support our contention that the ChRM was acquired during the cooling of the magma. The primary origin of the ChRM is also supported by a positive fold test on the Xiong'er data, and a coherent regional test between the results from the Taihang and Xiong'er areas. Two different site-mean directions were compiled from these new results along with previous publications. The first direction, from the Taihang and Xiong'er areas, yields Declination (D)/Inclination (I) = 12.4°/−3.7° (κ = 20.5, α_{95} = 4.3°, N = 57 sites). The second, from the Yinshan area is at (D) 36.7°/(I)−12.4° (κ = 86.8, α_{95} = 2.7°, N = 32 sites). We argue that the difference is due to Mesozoic and/or Cenozoic vertical-axis rotation of the Taihang and Xiong'er areas with respect to the fixed Yinshan-Ordos basin. The corresponding paleopoles for the Yinshan dykes falls at 245.2°E/35.5°N (A_{95} = 2.4°). A comparison between the NCC, Laurentia, Siberia and Baltica is consistent with possible links between these four blocks in a perhaps, even larger, continent. The proximity of Australia and India to the NCC is also evaluated.

1. Introduction

Although the proposition of a large Paleo-Mesoproterozoic supercontinent, named Columbia (or Nuna), was proposed more than a decade ago, its exact geometry, timing of amalgamation and timing of break-up are still contentious (Rogers, 1996; Meert, 2002, 2014; Rogers and Santosh, 2002; Zhao et al., 2002b; Pesonen et al., 2003, 2012; Zhao et al., 2004; Evans and Mitchell, 2011; Zhang et al., 2012a; Chen et al., 2013). As the only quantitative method to test the proposed configurations, systematic paleomagnetic studies of Paleo-Mesoproterozoic in different geological units are necessary. In spite of recent efforts to obtain reliable paleomagnetic data, the exact configuration of Columbia remains enigmatic.

The North China craton is one of the oldest regions in the world, but its location within Columbia is still unresolved although

* Corresponding author at: Institute of Geology and Geophysics, CAS, No. 19, Beitucheng Xilu, Chaoyang District, Beijing, China. Tel.: +86 10 82998418.
E-mail address: zhuiri2080@gmail.com (H. Xu).

http://dx.doi.org/10.1016/j.precamres.2014.10.004
0301-9268/

several distinct proposals were made on the basis of geological considerations. Li et al. (1996) suggested a Mesoproterozoic connection between Siberia and the NCC based on geological similarities in coeval sedimentary sequences found on both cratons. Condie (2002) proposed that the NCC–Siberia connection extended into the Paleoproterozoic, but placed the NCC against Northeastern Siberia to align the Trans-North China Orogenic belt to the Akitkan orogenic belt in Siberia. The resemblance between the NCC and Baltica was first proposed by Qian (1997). He noted the geological similarities between the Precambrian of both cratons. Although not particularly diagnostic, both Baltica and the NCC stabilized during the Archean, exhibited rifting in Proterozoic that formed trondhjemitic–tonalitic–granodioritc (TTG) along with supracrustals and a volcano-sedimentary sequence in the upper part of the sequence. Wilde et al. (2002) supported this relationship based on coeval collisions at ~1.8 Ga recorded by the Trans-North China Orogen (TNCO) and Kola-Karelian Orogen (Berthelsen and Marker, 1986; Wilde et al., 2002; Zhao et al., 2001). Based on evidence from coeval magmatic activity, Kusky et al. (2007a) proposed a linkage between the NCC, Baltica and Amazonia, placing the eastern margin of the NCC next to southwestern Baltica and the western side of the NCC against Amazonia. As major crustal formation in both the NCC and Southern India are coeval at 2.6–2.5 Ga indicated by granulite facies metamorphism, Kröner et al. (1998) proposed that the two blocks were connected as part of a single active continental margin. Based on the alignment of orogenic belts, Zhao et al. (2002a) presented the western and eastern blocks of the NCC adjacent to Northern India and Southern India respectively by assuming the TNCO and the Central India Tectonic Zone (CITZ) evolved together. Peng et al. (2005) used the geometry of coeval mafic dyke swarms in both the NCC and the Dharwar craton of India as evidence for a NCC–Dharwar connection. Based on similar evidences, Hou et al. (2008) slightly changed the relative positions and connected the NCC to the Cuddapah Basin at the eastern margin of the India.

Paleomagnetic data were also used to evaluate the NCC's proximity to other cratons in Columbia. Halls et al. (2000) suggested that the NCC, Laurentia and Siberia maintain an integral geometry similar to their present-day configuration in Columbia starting at ~1800 Ma based on apparent polar wander paths (APWPs) from the three blocks. Piper et al. (2011) placed the northern NCC next to western India based on the APWPs around 1800 Ma. Zhang et al. (2012a) also supported this connection based on the comparison of APWPs in Paleo-Mesoproterozoic. However, Chen et al. (2013) placed the southwestern part of the NCC to eastern India. Recently obtained poles from Amazonia were used to place the NCC between Baltica and Amazonia (Bispo-Santos et al., 2008, 2012, 2014; D'Agrella-Filho et al., 2012).

Based on these previous models, the position of the NCC within the Columbia supercontinent is ambiguous. In an effort to provide additional constraints on the position of the NCC, we report new data from coeval mafic dykes and the Xiong'er volcanics in the central NCC for a systematic and detailed paleomagnetic study, in order to solve the "where" and "when" problems discussed above.

2. Geological setting

Several proposals exist for the tectonic subdivisions of the NCC although there is a general consensus that it had stabilized by ~1800 Ma (Wu and Zhong, 1998; Wu et al., 1998; Zhai et al., 2000; Li et al., 2000; Kusky and Li, 2003; Zhao et al., 2005). Among these models, the tripartite division proposed by Zhao et al. (2005) is widely accepted. In that model, the Precambrian blocks (i.e. the Western and Eastern Blocks) evolved independently and collided along the trans-North China Orogen (Zhao et al., 2001, 2005; Li et al., 2000). The Western Block was formed by the amalgamation of the Ordos Block in the south and the Yinshan Block to the north along the east-west-trending Khondalite belt. Collision between the Western and Eastern Blocks occurred at either ~1.85 Ga (Wilde et al., 2002; Zhao et al., 2001, 2002a, 2005; Kröner et al., 2005; Guo et al., 2005) or ~2.5 Ga (Li et al., 2000; Kusky and Li, 2003). After cratonization, as a result of amalgamation of Archean blocks, the NCC experienced remobilization and recratonization (e.g. rifting, collision and/or uplift; Li et al., 2000; Zhai et al., 2000; Kusky and Li, 2003; Zhai and Liu, 2003; Kusky et al., 2007a, 2007b; Zhai and Peng, 2007; Li et al., 2010). During this remobilization, at least two significant magmatic events took place. This includes the emplacement of mafic dyke swarms in the central and western of the NCC, and the Xiong'er volcanics along the south margin during the Paleoproterozoic (Peng et al., 2008). Following these magmatic events, the NCC was covered by a thick sequence of Meso-Neoproterozoic (Changcheng, Jixian and Qingbaikou Systems) volcanic and sedimentary rocks (HBGMR, 1982).

The mafic dyke swarm investigated in this study is related to either break-up (and plume activity; Peng et al., 2008) or a post-NCC assembly extensional episode (Zhao et al., 2002b). Most of the mafic dykes trend NNW, are vertical or sub-vertical and can be up to 60 km in length and 100 m in width, with most around 15 m wide. The dykes extend more than 1000 km across the central NCC and are gabbroic in composition and doleritic in texture with sharp, chilled contacts with the country rocks. The primary textures show increasing hydrous alteration (including saussuritization of feldspar, conversion of pyroxene to amphibole, and serpentinization of olivine) toward the south (Qian and Chen, 1987; Halls et al., 2000; Hou et al., 2001; Peng et al., 2005, 2008). The dykes in the Yinshan and Taihang areas are dated at around ~1780 Ma (Fig. 1 and Table 1) (Halls et al., 2000; Li et al., 2001; Wang et al., 2004; Peng et al., 2005, 2006).

The Xiong'er volcanics have a thickness of 3–7 km and extend in outcrop over an area of 60,000 km^2. The volcanic rocks are exposed in the Zhongtiao, Xiao, Xiong'er and Waifang Mountains and consist of lava and pyroclastic rocks interlayered with minor sedimentary rocks (Zhao et al., 2002b). Stratigraphically (from oldest to youngest) these rocks are subdivided into the Xushan Formation (Fm.), Jidanping Fm. and Majiahe Fm. The basal Xushan Fm. is composed of basaltic andesite and andesite with minor dacite, dacitic rhyolite, and basalt. The Jidanping Fm. contains dacite-rhyolite flows interbedded with basaltic andesite and andesite. The Majiahe Fm. is composed of basaltic andesite and andesite interlayered with voluminous sediments and pyroclastic rocks and minor rhyolite (Zhao et al., 2002b). The duration of volcanic activity related to the emplacement of the Xiong'er rocks was discussed by several authors (Table 1) (Zhao et al., 2004; He et al., 2009; Cui et al., 2010; Wang et al., 2010). The reported ages for Majiahe Fm. and Xushan Fm. are indistinguishable within uncertainty at around 1780 Ma (Fig. 1). Based on these data, we consider the paleomagnetic pole from the Xiong'er volcanic rocks as contemporary with the mafic dykes to its north.

3. Paleomagnetic experiments and results

3.1. Paleomagnetic sampling

Standard oriented cylindrical cores were collected with a portable, gasoline-powered rock drill from 18 sites (dykes) in the Yinshan area in Inner Mongolia, 27 sites (dykes) in the Taihang area of Shanxi and Hebei, and 26 sites (lavas) of the Xiong'er volcanics in the Xiaoshan area of Henan. The distribution of paleomagnetic sampling sites is shown in Fig. 1. Samples were oriented using both a sun and magnetic compass. Every core was cut into a single

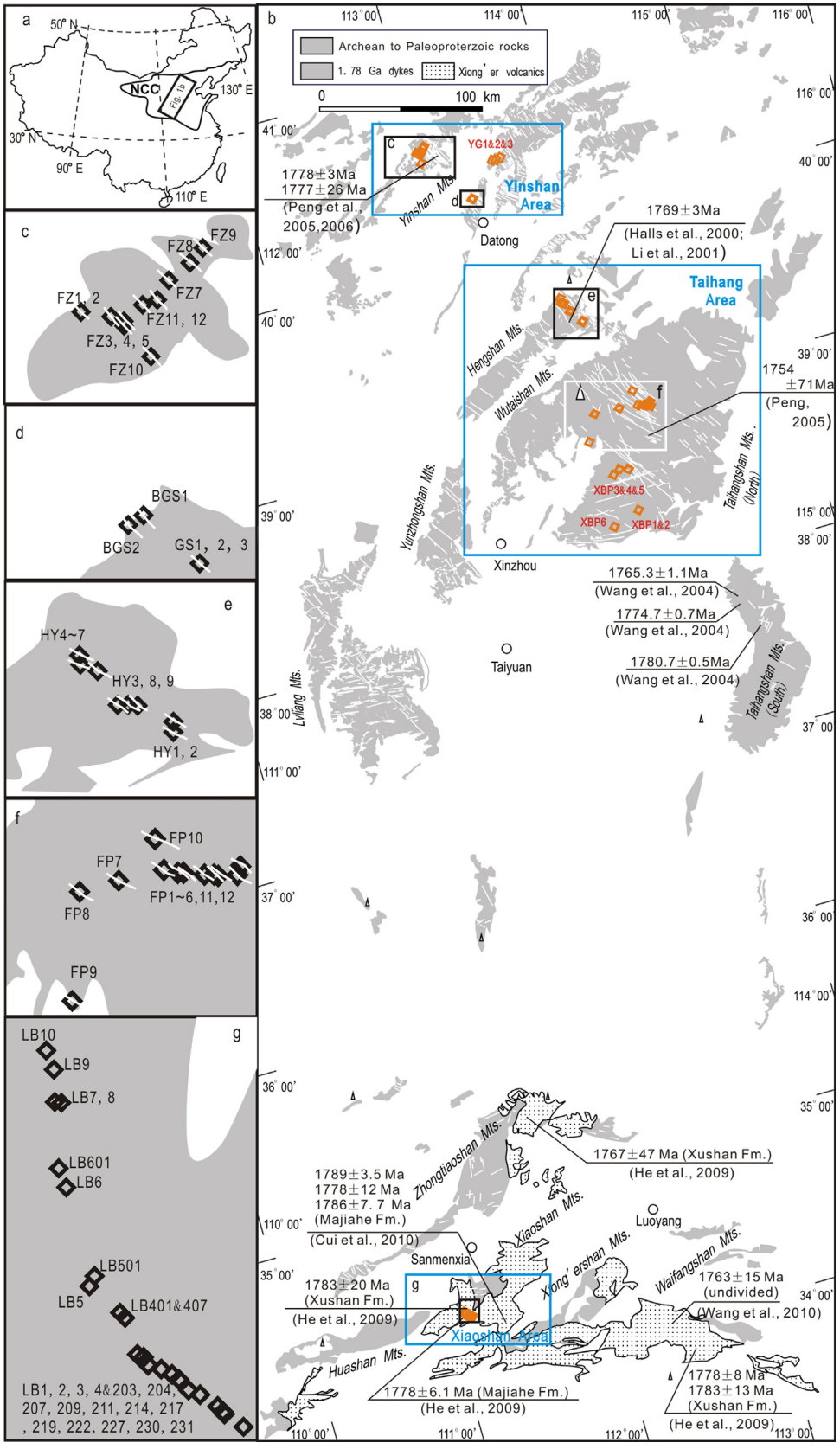

Fig. 1. (a) The location of the NCC in China. (b) Simplified geological maps of the mafic dykes and the Xiong'er volcanics. Paleomagnetic sampling sites are shown with open diamonds. Extant geochronologic data are also presented together with their references. (c)–(g) Expanded visions from the squares presented in (b) to show detailed regional distribution of the sites. The white lines represent mafic dykes.

Modified from Peng et al. (2008).

Table 1
A summary of reported ages from Yinshan and Taihang dykes and Xiong'er volcanic rocks.

Rocks	Ages (Ma)	Method	Ref.
Yinshan dykes	1778 ± 3	Zircon SHRIMP U-Pb	Peng et al. (2005)
	1777 ± 26	Baddeleyite ID-TIMS U-Pb	Peng et al. (2006)
Taihang dykes	1769 ± 2.5	Zircon ID-TIMS U-Pb	Halls et al. (2000), Li et al. (2001)
	1754 ± 71	Baddeleyite ID-TIMS U-Pb	Peng et al. (2006)
	1780.7 ± 0.5, 1765.3 ± 1.1, 1774.7 ± 0.7	Whole rock Ar-Ar	Wang et al. (2004)
Xiong'er volcanic rocks			
Majiahe Fm.	1789 ± 3.5	Baddeleyite Cameca SIMS	Cui et al. (2010)
	1778 ± 12, 1786 ± 7.7	Zircon Cameca SIMS	Cui et al. (2010)
	1778 ± 6.1	Zircon LA-ICP-MS U-Pb	He et al. (2009)
Xushan Fm.	1783 ± 20, 1783 ± 13, 1767 ± 47	Zircon SHRIMP U-Pb	He et al. (2009)
	1778 ± 8	Zircon LA-ICP-MS U-Pb	He et al. (2009)
Undivided	1763 ± 15	Zircon LA-ICP-MS U-Pb	Wang et al. (2010)

specimen and a pilot selection of samples was used to determine the best method of demagnetization.

3.2. Rock magnetic results

In order to identify the magnetic carriers, rock magnetic tests were carried out on selected samples. Hysteresis experiments were conducted in a MicroMag Vibrating Sample Magnetometer, and thermomagnetic analysis of magnetic susceptibility (κ–T curves) using a CS-4 apparatus coupled to a KLY-4s Kappabridge instrument in the Paleomagnetic and Geochronology Laboratory of the IGGCAS.

Narrow-waist hysteresis curves were obtained from the samples from the Yinshan and Taihang areas, with low coercivity (Fig. 2a and b). IRM acquisition curves (Fig. 2c) are practically identical, reaching the saturation remanent magnetization in fields below 0.3 T, consistent with a dominance of low-coercivity grains. Most samples plotted in the pseudo-single domain (PSD) field in day diagrams (Fig. 2d; Dunlop, 2002a,b). κ–T curves yielded from these samples show Curie temperatures around 580 °C and a pronounced Hopkinson peak (Fig. 3). All these characteristics indicate the interpretation of PSD magnetite and titanomagnetite is the main remanence carrier in these rocks.

The main remanence carrier in most of samples from the Xiaoshan area is magnetite (Fig. 4a–d). A rather limited number of samples exhibit wasp-waisted curves, that have been interpreted as resulting from two components with overlapping coercivity (Fig. 4e; Roberts et al., 1995). The κ–T curves of such samples show decrease from ~580 °C to ~680 °C (Fig. 4f), also suggesting the coexistence of hematite and little magnetite.

3.3. Demagnetization methods

All samples were submitted to stepwise thermal demagnetization in the Paleomagnetism and Geochronology Laboratory in Institute of Geology and Geophysics, Chinese Academy of Sciences. Measurement of remanent magnetization was conducted on a 2G Enterprise SQUID magnetometer. These instruments are housed in a magnetically shielded room with ambient field <300 nT. Thermal demagnetization was carried out in a ASC TD-48 oven with steps of 50 °C or 100–500 °C and reduced to 10 °C or 20 °C, sometimes even 2 °C for some samples because their intensities decrease sharply above 520–580 °C. Samples that were not demagnetized by 580 °C were treated to 680 °C using 10 °C steps. Magnetic components for each specimen were analyzed in the orthogonal plots (Zijderveld, 1967), and directional data were calculated using principal component analysis (Kirschvink, 1980). At least five demagnetization steps (including the origin point) were used to calculate vectors, and an upper limit for mean angular deviation (MAD) of 10° was used. Most samples of the northern NCC had MAD's < 5°. Fisher's (1953) statistics were used to calculate site-mean directions.

3.4. Paleomagnetic results

Of eighteen sites from the Yinshan area (excluding site GS3 which was collected for a baked contact test), sixteen yielded consistent and stable directions. Results from site YG3 were problematic. Although individual specimen behavior was stable, high temperature directions obtained from linear trajectories were scattered at the site level. Mean direction of YG2 is significantly different from other sites (Fig. 5a). These two sites were excluded for further consideration. At other sites, as many as three components could be isolated in the Zijderveld plots (Fig. 6a and b). The mean direction of the low-temperature component (LTC, NRM-200 °C) is identical to the present geomagnetic field direction (Mean: $D/I = 353°/+66°$, $\alpha_{95} = 6.1°$, Fig. 7a). Intermediate-temperature components (200–500 °C) were only found in a small number of the samples. The mean direction of $D/I = 12°/46°$ ($\kappa = 14$, $\alpha_{95} = 13.3°$, $n = 9$ samples) resembles the late Mesozoic direction for the NCB, suggesting a late Mesozoic remagnetization. The high-temperature mean component (HTC) was generally isolated above 500 °C and yielded a mean declination of 36°, inclination of −5° ($\kappa = 63$, $\alpha_{95} = 4.7°$, $N = 16$ sites) (Fig. 7b). A summary of paleomagnetic results from the Yinshan area are presented in Table 2.

A ~1320 Ma diabase porphyry dyke (site GS3; Peng, 2014) intruded to the dykes GS1 and GS2 was used to perform an inverse baked contact test. Samples from GS1 and GS2 were collected at various distances from the contact with GS3. The mean direction calculated from dyke GS3 was $D/I = 89°/+29°$ ($\kappa = 47$, $\alpha_{95} = 6°$, $n = 15$ samples). Samples of GS1 and GS2 collected within the baked zone show similar directions to those observed in dyke GS3 (i.e. baked GS1 and GS2: $D/I = 106°/+31.7°$, $D/I = 106.6°/+36.4°$). Samples distant from the contact with GS3 yielded magnetization directions very similar to those reported above for the older dykes (unbaked GS1 and GS2: $D/I = 49.9°/-1.2°$, $D/I = 42.4°/-2.4°$) (Fig. 8). Although the baked test can only prove the ChRM of the dyke GS3 primary, the difference in directions is supportive of our assertion that the magnetic directions reported in the older dykes may also be primary.

Paleomagnetic results from samples collected in the Taihang area were complicated. According to our strict criteria of accepting results where the MAD < 10° for specimen directions and $\alpha_{95} < 15°$ for site means, only 13 of 27 sites were selected to calculate the mean direction. The mean of LTCs below 200 °C (349.9°/+61.5°, $\alpha_{95} = 3.9°$) lies next to the direction of PGF (354.5°/+57.7°) (Fig. 9a). Characteristic remanence was isolated above 500°C (Fig. 6c and d). The site-mean direction is $D/I = 16°/+1°$ ($\kappa = 24.8$, $\alpha_{95} = 8.5°$, $N = 13$ sites) (Table 3). Two sites showed an antipodal direction. Although the number of reversed-direction dykes is too small to provide a

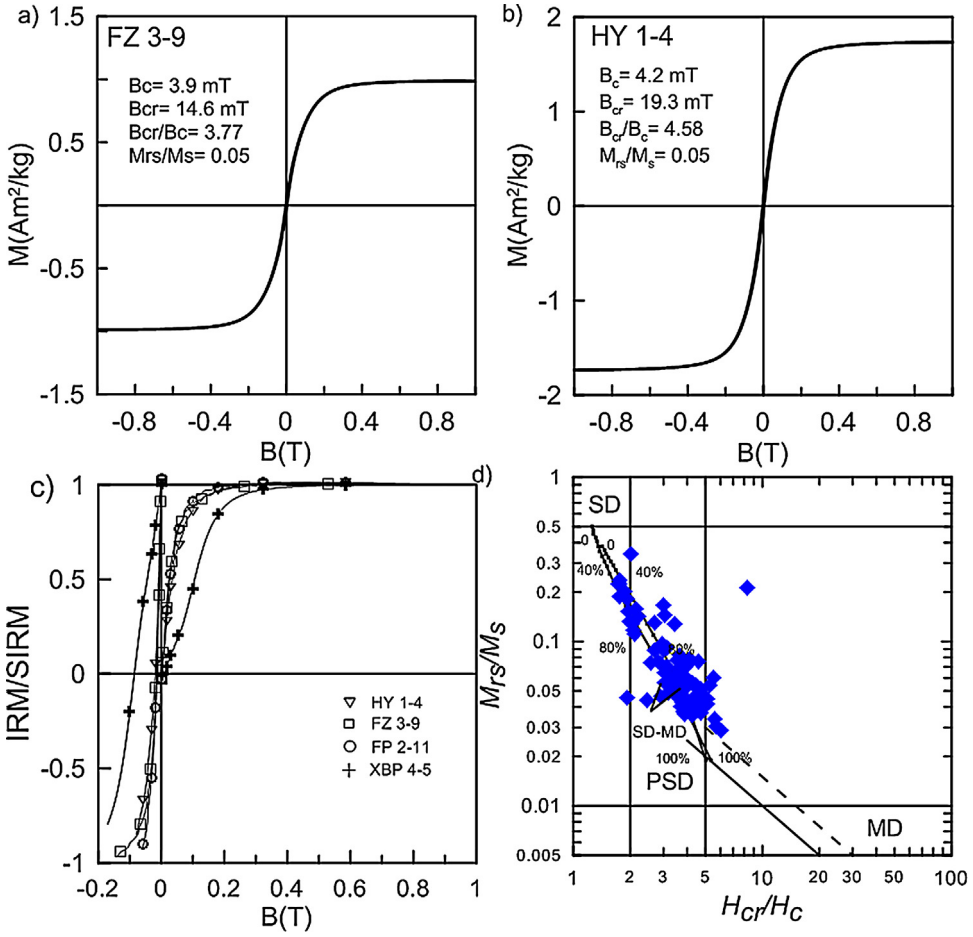

Fig. 2. Room-temperature rock magnetic analysis of selective samples from the Yinshan and Taihang dykes. (a, b) Hysteresis curves with narrow waist saturate below the field of 300 mT, indicating the presence of titanomagnetite or magnetite. (c) Acquisition and demagnetization curves of isothermal remanent magnetization (normalized intensities versus magnetic field). (d) Day diagram shows most samples fall along a trend parallel to the theoretical SD–MD magnetite mixing curves (Dunlop, 2002a,b), the percentage shows the relative concentration of MD (SD: single domain, PSD: pseudo single domain, MD: multidomain).

rigorous reversal test, it does provide some additional evidence that the remanence in these dykes may be primary (Fig. 9b). For the remaining fourteen sites, five showed only present geomagnetic field directions (Fig. 5b) and five had no stable directions (Fig. 5c). The remaining four sites are discussed below.

We carried out baked-contact tests in two dykes in the Taihang area, HY5 and FP9 that intrude the Archean-age tonalite–trondhjemite–granodiorite (TTG) in the Hengshan and Wutaishan Mtns. Samples were collected from both the dykes and the surrounding TTG rocks. Unfortunately, neither the dyke at Site HY5 nor the host rocks yielded consistent directions. A stable remanence was isolated from samples collected at the margin of dyke FP9. These samples from the baked country rock yielded stable directions that are similar with those of FP 9 (Fig. 10). The results are not conclusive because the unbaked country rocks showed an unstable remanence, nevertheless, the consistency between the

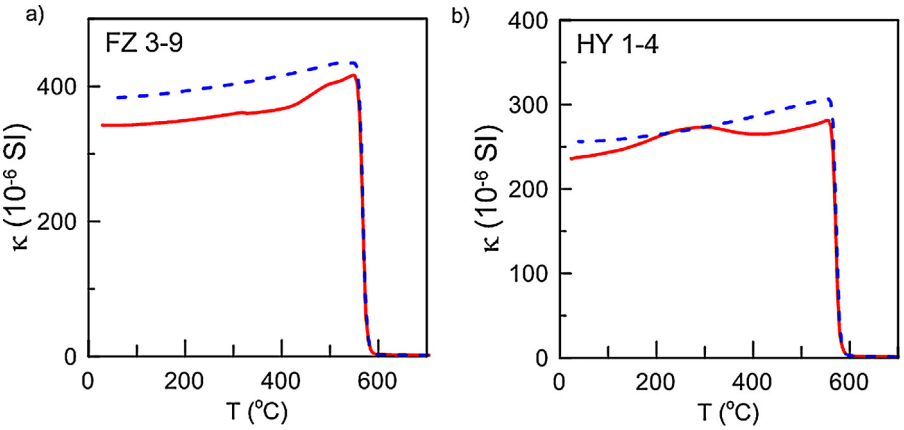

Fig. 3. Thermomagnetic curves of selective samples from the Yinshan and Taihang dykes showing variation in magnetic susceptibility with significant decrease around 580 °C.

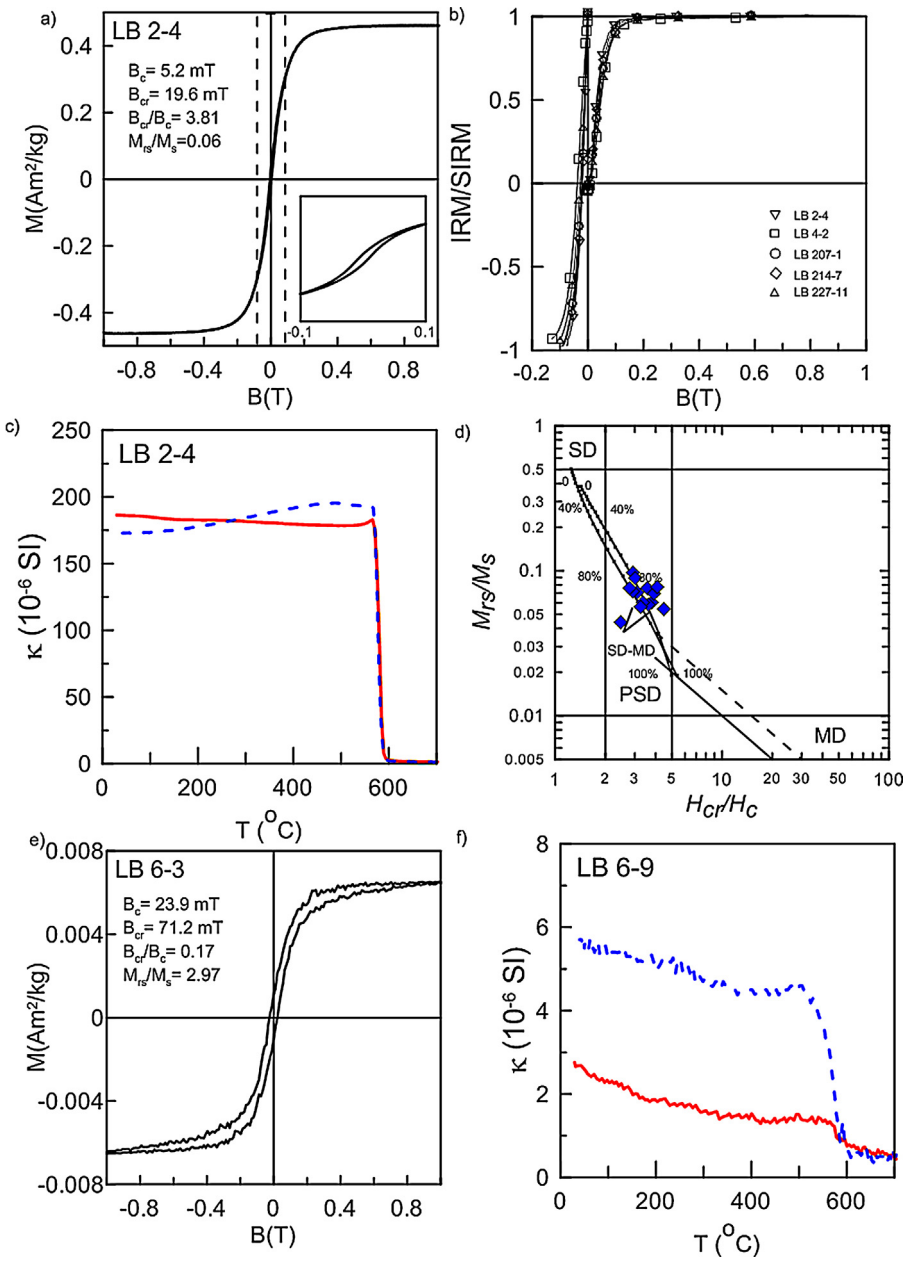

Fig. 4. Rock magnetic results from Xiaoshan area. (a–d) Systematic analyses indicate magnetite is the main magnetic carrier. (e–f) shows the co-existence of hematite and little magnetite in these samples.

baked samples and the dyke are suggestive of a positive baked contact test for the ChRM of FP9. The direction recorded in FP9 is distinguished from other 1780 Ma dykes in the Taihang area. Three other dykes in the region have similar ChRM with FP9 and their site-mean direction is $D = 80°$, $I = +42°$ ($\kappa = 65$; $\alpha_{95} = 11.5°$, $N = 4$ sites).

We collected 26 lava flows from the Xiong'er volcanic rocks (Xushan Formation) near the Xiaoshan Mtns. in Henan province. The outcrop is continuously exposed along a road near Lingbao County for over 10 km. The dominant rock types are basalt and andesite that are interbedded with purple mudstones. A low temperature direction similar to the present geomagnetic field was isolated at temperatures below 200 °C (345.6°/+51.4°, $\alpha_{95} = 3.5°$; Fig. 11a). The HTCs were isolated above 500°C (Fig. 6e and f). We only chose those sites with at least 4 candidate samples to calculate the site-mean direction. The site-mean direction of the higher-temperature component is $D/I = 0.7°/-14°$ ($\kappa = 28.8$; $\alpha_{95} = 9.8°$, $N = 8$ sites; Fig. 11b; Table 4). Two sites (including three lavas, sites LB2 and LB203 were combined into one site) showed antipodal directions and the existence of a dual-polarity magnetization within the volcanic rocks suggests the HTC was acquired during lava cooling. Samples from fifteen sites were rejected for that they record single PGF-like component or did not show stable directions (Fig. 5d and e).

We employed the method of Biggin et al. (2008) to evaluate secular variation within our three study areas. S_B values obtained were 9.3° for the Yinshan area, 13.0° for the Taihang area and 8.5° for the Xiaoshan area. Compared to the S_B value over the past 5 Myr, the result from the Taihang area shows a comparable PSV pattern. Though the PSV of Xiaoshan area is slightly lower than the idealized model, the existence of reversals demonstrates that the remanence acquisition was long enough to average out the secular variation. Only a single polarity was observed in the Yinshanarea and the value of S_B was lower than expected. We note that the site mean

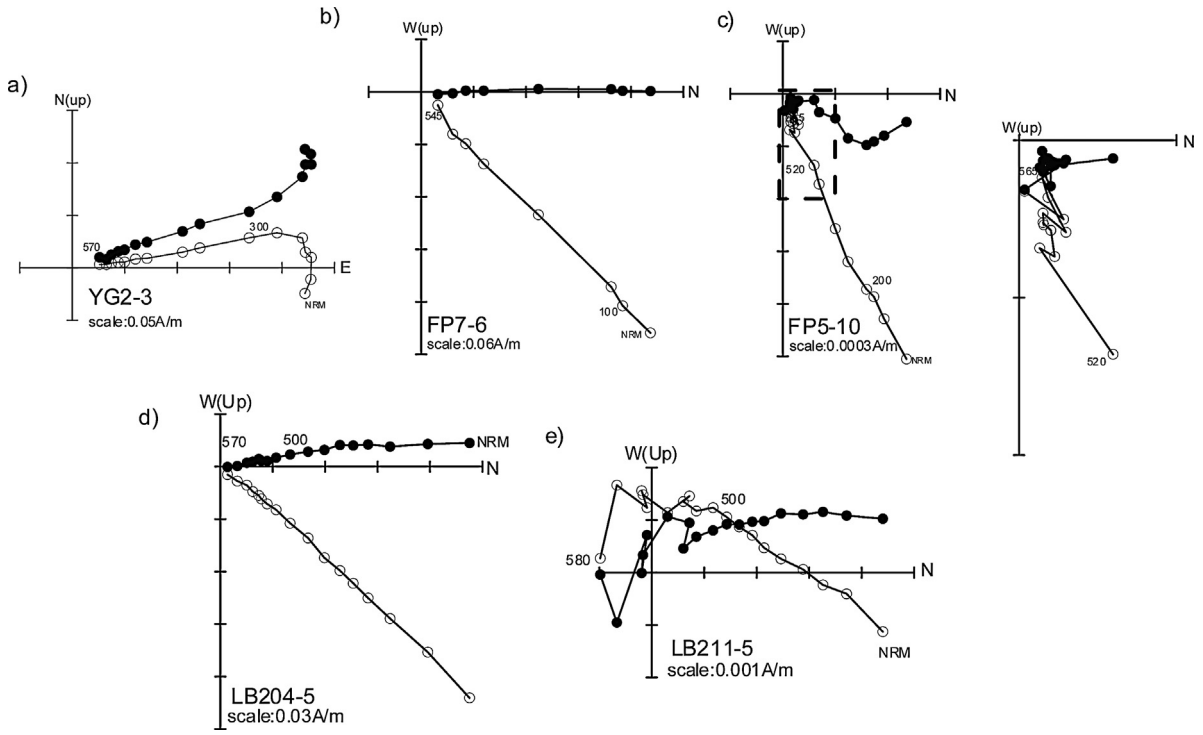

Fig. 5. Selective demagnetization curves of the disturbed samples from (a) the Yinshan area, (b, c) from the Taihang area and (d, e) from the Xiaoshan area. Open/closed dots in the vector plots denote vertical/horizontal projections.

directions are calculated from sixteen different dykes separated by a wide distance and therefore secular variation is likely averaged.

4. Discussion

4.1. Proterozoic paleomagnetic poles from the NCC

A number of previous paleomagnetic studies were carried out on the mafic dyke swarms and Xiong'er volcanic rocks of the NCC. Previously published directions show three different paleomagnetic poles from the Yinshan, Taihang and Waifangshan areas (Halls et al., 2000; Piper et al., 2011; Zhang et al., 2012a; Figs. 12 and 13). Two groups of magnetic directions were found from the dykes in the Yinshan and Taihang areas, in which the difference was attributed to the cooling sequence resulted from the various intrusion depths (Piper et al., 2011). However, other hypotheses remain viable due to the limited data available. This study extended the sampling area and collected as many sites as possible to solve the problem.

Our result from 16 dykes in the Yinshan area ($D/I = 36^\circ/-5^\circ$, $\kappa = 63, \alpha_{95} = 4.7$) is comparable with Halls et al. (2000). In total, there are four contact baked tests to support a primary ChRM in the Yinshan area. Although pointed out in Halls et al. (2000), the results from these dykes overlaps with a reported Paleozoic pole from the Alashan terrane of the NCC (Zhao et al., 1993), the later was considered from an allochthonous terrane that amalgamated to the NCC by the late Triassic (Yuan and Yang, 2014). The data from sixteen

Table 2
Paleomagnetic results from the Yinshan area. Slat, Slon: sample locality latitude and longitude; Trend, Dip: attitude of dykes; n/N = number of used/demagnetized samples; Dg, Ig: site mean declination, inclination; κ = precision parameter of Fisher (1953); α_{95}: radius of the 95% confidence circle about the mean direction; Sites labelled with * are not included in the calculation of site-mean direction. Dashes indicate no trend or dip was obtained from field work, or no stable HTC can be isolated during thermal demagnetization.

Site	Slat (°N)	Slon (°E)	Trend (°)	Dip (°)	n/N	Dg (°)	Ig (°)	κ	α_{95} (°)
FZ1	40.578	112.986	345	90	13/14	27.8	−0.6	32.2	7.4
FZ2	40.578	112.986	350	90	16/16	32.3	−2.9	391	1.9
FZ3	40.573	112.992	–	–	14/16	41.3	−1.9	130	3.5
FZ4	40.574	112.992	–	–	15/15	28.6	−3.6	341	2.1
FZ5-1	40.575	112.991	–	–	20/20	43.4	−6.1	319	1.8
FZ5-2	40.575	112.991	–	–	9/9	22.1	1.7	459	2.4
FZ6	40.600	113.052	352	90	14/15	44.6	−11	84.4	4.4
FZ7	40.600	113.052	352	90	5/17	16.5	−2.6	89.5	8.1
FZ8	40.590	113.043	350	90	13/14	46.5	−4.1	714	1.6
FZ9	40.572	113.025	–	–	14/14	41.4	−9.9	363	2.1
FZ10	40.515	113.000	355	90	18/18	39.6	−4.7	332	1.9
FZ11	40.563	113.006	355	90	12/14	34.2	−8.5	310	2.5
FZ12	40.562	113.008	355	90	18/18	31.7	−4.3	35.5	5.9
BGS1	40.241	113.297	340	90	16/16	49.9	−1.2	13.4	10.5
BGS2	40.241	113.297	340	90	7/7	42.4	−2.4	66.7	7.4
YG1	40.388	113.586	348	90	14/15	40.9	−15	110	3.8
YG2*	40.384	113.590	355	–	9/10	67.9	−12	27.0	10.1
YG3	40.376	113.650	–	–	–	–	–	–	–
Site-mean					16	36.4	−4.9	63	4.7

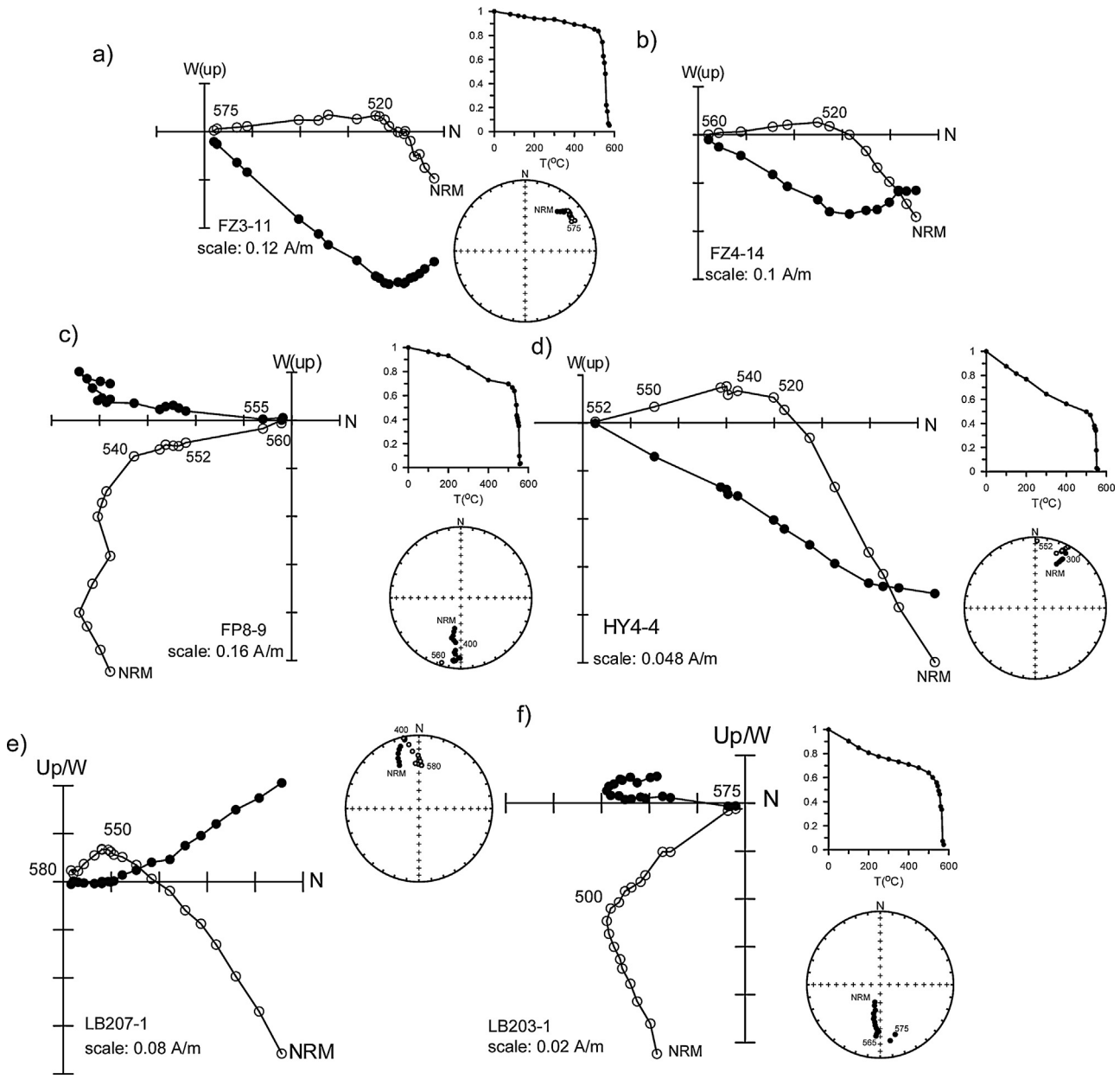

Fig. 6. Stepwise thermal demagnetization of representive samples from (a, b) the Yinshan area, (c, d) the Taihang area and (e, f) the Xiaoshan area. Figure shows orthogonal projections (open/closed dots in the vector plots denote vertical/horizontal projections), normalized intensity curves (J/J_0 versus demagnetization temperature (T) curves) and equal-area projections (closed/open circles represent downward/upward pointing magnetizations). All the orthogonal plots and equal-area projections are drawn in geographic coordinates.

Yinshan dykes in Halls et al. (2000) were combined with our results and yield a grand mean with $D/I = 36.7^\circ/-12.4^\circ$ ($\kappa = 86.8$, $\alpha_{95} = 2.7^\circ$, $N = 32$ sites). All the directions have been recalculated to the same reference location (36°N/112°E).

Samples in the Taihang area were collected from Shanxi and Hebei Provinces with a site-mean direction of 13 dykes at $D/I = 16^\circ/+1^\circ$ ($\kappa = 24.8$, $\alpha_{95} = 8.5^\circ$). Three dykes (GU9, GU12, GU26) in the Taihang area were reported by Halls et al. (2000). Although GU12 and GU26 became more clustered with other site-mean directions in the Yinshan area after structural correction (SC), we group them with the results from the Taihang area and the directions show better clustering without SC suggesting that the small deviations from vertical are not due to younger tilting. Paleomagnetic directions of another nineteen dykes in the Taihang area (including South Taihangshan area) were from Piper et al. (2011). A grand mean of these results yields a direction of $D/I = 12.5^\circ/-3.1^\circ$ ($\kappa = 20$, $\alpha_{95} = 5.6^\circ$, $N = 35$ sites) for a reference locality at 36°N/112°E. Directional data from four dykes (including FP9) are distinctly different from the 1780 Ma ChRM and published Phanerozoic directions from the NCC. It is possible that they are Precambrian in age. Piper et al. (2011) also reported an undated Precambrian Component B that is younger than ~1.8 Ga. However, the uncertain ages of these two components preclude a more detailed tectonic interpretation.

The Xiong'er volcanic rocks in this study were collected in Xiaoshan area. Eight lavas from Xushan Fm. yielded a direction at $D/I = 0.7^\circ/-14^\circ$ ($\kappa = 28.8$, $\alpha_{95} = 9.8$). Zhang et al. (2012a) reported paleomagnetic results from 14 lavas in both Xushan and Majiahe Fm. in Waifangshan area. As the two formations are of similar ages, the directions from both Xushan and Majiahe Fm. were combined to yield a mean $D/I = 12.3^\circ/-4.7^\circ$ ($\kappa = 20.5$, $\alpha_{95} = 7^\circ$, $N = 22$ sites) for a reference location at 36°N/112°E.

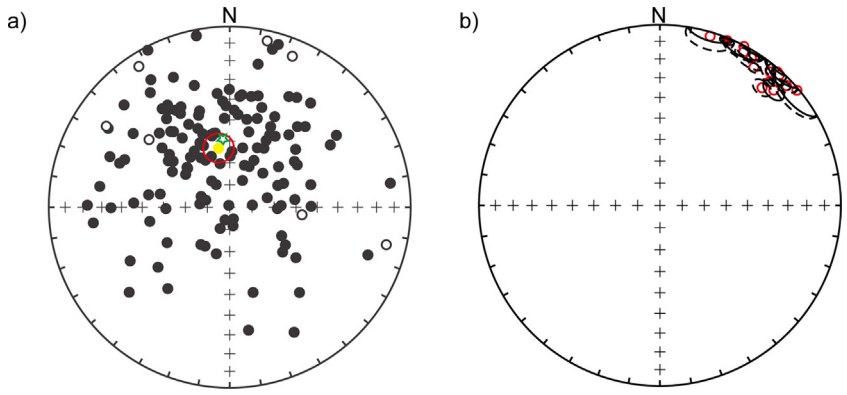

Fig. 7. Equal-area projections of directions isolated in the Yinshan dykes. (a) Low-temperature components of samples. Yellow dot with 95% confidence circle indicates the group mean. Open star denotes the present geomagnetic field direction (PGF); (b) site mean high-temperature components. Open (closed) circles represent downward/upward pointing magnetizations. (For interpretation of reference to color in this figure legend, the reader is referred to the web version of this article.)

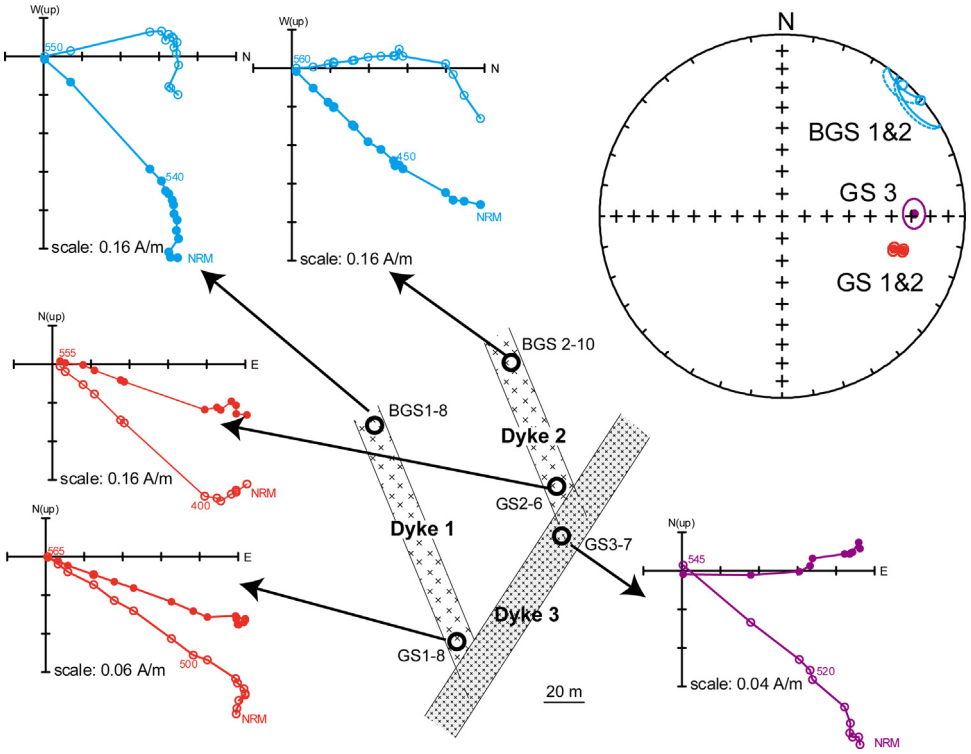

Fig. 8. An inverse baked contact test in the Yinshan area. Dyke GS3 is younger than Dyke GS1 and Dyke GS2 as it intruded into the latter two dykes. The baked samples of older dykes show similar directions with GS3 while the unbaked ones show consistent directions with the rest coeval mafic dykes in the Yinshan area. A bar scale is given to tell the width of dykes and distance of sampling positions from GS3.

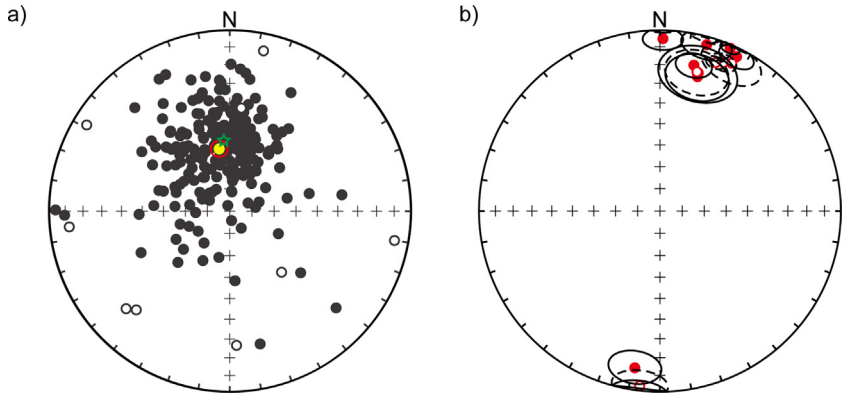

Fig. 9. Equal-area projection plots of directions isolated in the dykes in the Taihang area in this study. (a) Low-temperature components of samples. (b) Site mean high-temperature components. Symbols are as for Fig. 7.

Table 3
Paleomagnetic results from the Taihang area. Sites labelled with [a] are not included in the calculation of site-mean direaction. Dashes indicate no trend or dip was obtained from field work, no stable HTC or PGF-like directions. See Table 2 caption for other notes.

Site	Slat (°N)	Slon (°E)	Trend (°)	Dip (°)	*n*/*N*	Dg (°)	Ig (°)	κ	α_{95} (°)
XBP1	38.559	113.870	325	76.5E	5/10	13.1	18.3	132	6.7
XBP2	38.559	113.871	275	77E	–	–	–	–	–
XBP3	38.575	113.805	320	76.5E	6/9	15.6	23.9	30.9	12.2
XBP4	38.329	113.862	323	76.5E	9/10	187	−3	32.6	9.2
XBP5[a]	38.555	113.755	340	85 W	8/10	80.9	39.6	111	5.3
XBP6[a]	38.284	113.655	–	–	8/12	80.5	54	137	4.7
FP1	38.852	114.158	340	85E	–	–	–	–	–
FP2	38.863	114.127	330	75E	4/6	15.7	5	116	8.6
FP3	38.867	114.114	340	61E	6/12	15.5	21.8	21	15
FP4	38.864	114.126	330	75E	7/12	1	5.2	82.4	6.7
FP5	38.873	114.095	–	–	–	–	–	–	–
FP6	38.878	114.068	335	80E	8/10	23.1	−12	135	4.8
FP7	38.895	113.927	315	75SW	–	–	–	–	–
FP8	38.907	113.738	343	81E	7/12	189	13.2	42.1	9.4
FP9[a]	38.768	113.644	336	79E	13/13	86.6	32.5	305	2.4
FP10	38.962	114.057	295	70E	7/9	26.4	5.3	96.9	6.2
FP11	38.875	114.159	310	–	–	–	–	–	–
FP12	38.866	114.145	315	88E	4/12	14.9	−21	59.7	12
HY1	39.413	113.841	330	85E	7/7	20.5	−13	317	3.4
HY2	39.409	113.835	336	85E	–	–	–	–	–
HY3	39.484	113.769	343	85E	–	–	–	–	–
HY4	39.569	113.725	345	73E	4/6	25.9	−10	70.6	11
HY5	39.544	113.723	329	85E	–	–	–	–	–
HY6[a]	39.544	113.723	326	72E	11/11	71.9	41.1	402	2.3
HY7	39.537	113.740	345	76E	11/12	23.3	2.2	208	3.2
HY8	39.486	113.771	346	86E	–	–	–	–	–
HY9	39.487	113.773	331	84E	–	–	–	–	–
Normal polarity					11	17.8	2.3	23.6	9.6
Reversal polarity					2	188	5.1	49	36.5
Site-mean					13	16.2	1.2	24.8	8.5

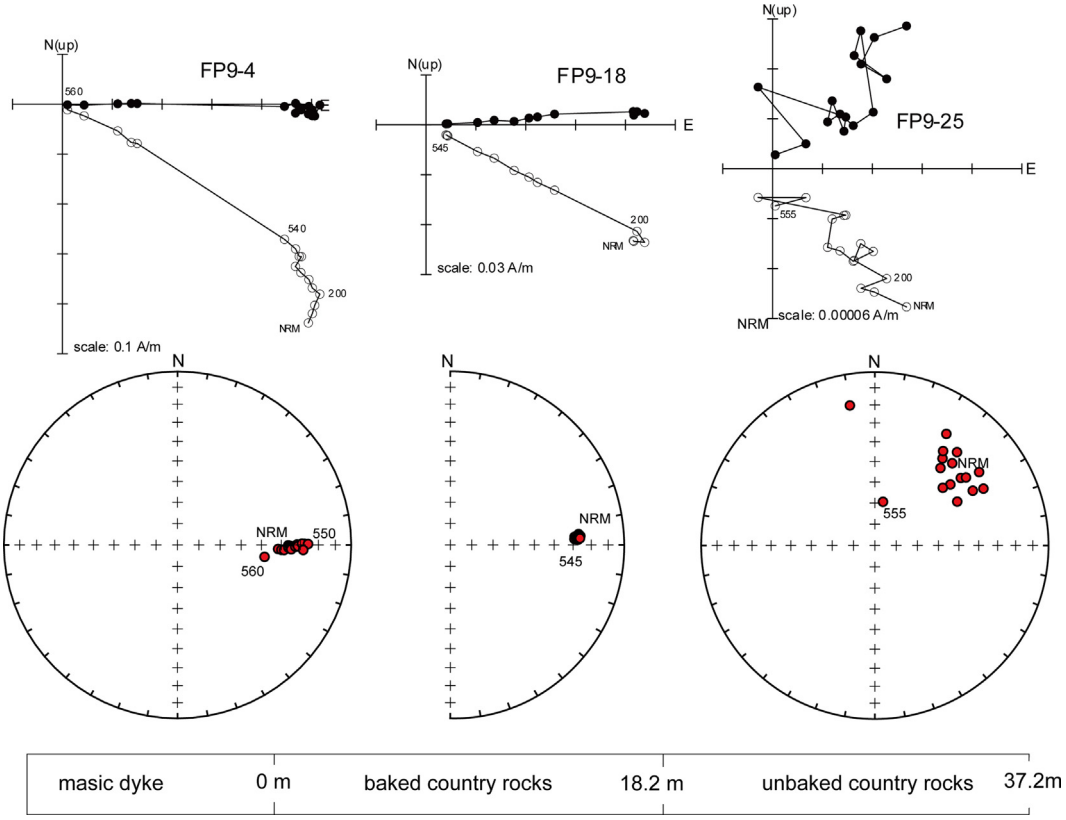

Fig. 10. A partially positive baked contact test was conducted on dyke FP9 (width ~ 40 m) in the Taihang area. Unbaked country rocks (18.2–37.2 m away from contact margin) do not have a stable HTC. Baked country rocks (0–18.2 m away from contact margin) have similar HTC with the dyke.

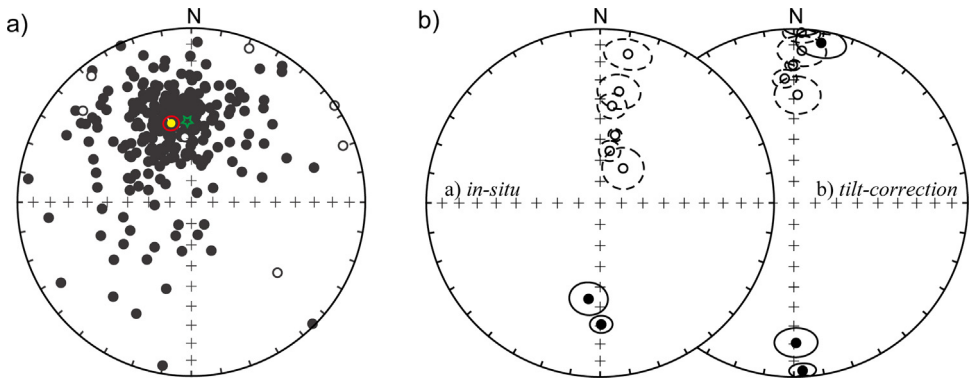

Fig. 11. Equal-area projections of directions isolated in the Xiong'er Volcanic rocks. (a) Low-temperature components of samples. (b) Site mean high-temperature components in situ (left) and after bedding correction (right). Symbols are as for Fig. 7.

These site-mean directions give a positive fold test at 95% confidence limit ($\xi_{\text{in situ}} = 11.2 > \xi_{\text{critic value}} = 5.4 > \xi_{\text{tilt-corrected}} = 0.02$) (McFadden, 1990). The folds are probably formed by the collision between the North China and South China Blocks in the Mesozoic (Meng and Zhang, 1999; Yang and Besse, 2001). So the ChRM obtained should be at least older than Mesozoic time. The similarity between the results of the Xiong'er and Taihang areas lead us to calculate a grand mean at $D/I = 12.4^\circ/-3.7^\circ$ ($\kappa = 20.5$, $\alpha_{95} = 4.3$, $N = 57$ sites) and it can pass a regional fold test of McFadden's (1990) at 95% confidence limit ($\xi_{\text{in situ}} = 19.1 > \xi_{\text{critic value}} = 8.8 > \xi_{\text{tilt-corrected}} = 2.42$).

According to the results discussed above, we note that the virtual geomagnetic poles (VGPs) of these three areas scatter along a small-circle trend centered in the sampling areas (Fig. 14). This form of scatter might also imply relative rotations between the Yinshan and Taihang areas. The two regions rest on distinct crustal blocks that are separated by Cenozoic rifts (Deng and Zhang, 2002). The Taihang area has been deduced to experience a ~10–20° counter-clockwise rotation relative to the Ordos Block in the Mesozoic and/or Cenozoic (Shi et al., 2004; Zhang et al., 2003; Huang et al., 2005). The early Jurassic paleomagnetic pole from the Yinshan area overlaps with a coeval pole from the Odors Block (Uno and Huang, 2003; Yang et al., 1992), indicating the two blocks remained relative stable since the mid-Mesozoic. Based on these results, we consider that the paleomagnetic direction from the Yinshan area may better represent the NCC. Using a 20° clockwise vertical axis rotation, the directions from the Taihang and Xiong'er areas align with those of the Yinshan area (Fig. 13b). The resulting pattern supports the geometry of a giant mafic dyke swarm pattern in the NCC (Peng et al., 2006; Peng, 2010). Taking the uncertainty of exact values of local rotation into account, we only consider the result from the Yinshan area as a high-quality paleomagnetic pole at 245.2°E, 35.5°N ($\kappa = 109.5$, $A_{95} = 2.4^\circ$, $N = 32$ sites) that yields a $Q = 6$ according to the criteria of Van der Voo (1990).

Table 4
Paleomagnetic results from the Xiaoshan area. The Section is located at 34.4°N/111.0°E. Dg(Ds), Ig(Is): declination and inclination before (and after) tilt correction. See Table 3 caption for other notes.

Site	Direction of dip	Dip (°)	*n*/*N*	Dg (°)	Ig (°)	Ds (°)	Is (°)	κ	α_{95}(°)
LB1	165	15	–	–	–	–	–	–	–
LB2&203	162	28	14/24	179.5	30.8	177	3.9	75.5	4.6
LB204	164	30	–	–	–	–	–	–	–
LB207	171	42	5/9	7	−43.2	2.6	−2.3	147	6.3
LB209	163	38	10/10	12.4	−57.2	360	−21.8	268	3
LB211	163	38	–	–	–	–	–	–	–
LB214	163	38	10/11	10.4	−65.2	356	−29.1	97.9	4.9
LB217	177	41	–	–	–	–	–	–	–
LB219	163	38	–	–	–	–	–	–	–
LB222	163	38	–	–	–	–	–	–	–
LB227	163	38	5/12	33.6	−70.6	2	−37.8	63.1	9.7
LB230	163	38	–	–	–	–	–	–	–
LB231	163	38	–	–	–	–	–	–	–
LB3	153	26	–	–	–	–	–	–	–
LB4	153	26	7/13	9.6	−35.3	3	−13.4	45.5	9
LB41	151	46	–	–	–	–	–	–	–
LB47	150	46	–	–	–	–	–	–	–
LB5	155	26	–	–	–	–	–	–	–
LB51	150	43	–	–	–	–	–	–	–
LB6	155	26	13/20	10.6	−14	9.7	7.4	22.9	8.9
LB61	155	26	–	–	–	–	–	–	–
LB7	156	44	–	–	–	–	–	–	–
LB8	155	26	–	–	–	–	–	–	–
LB9	155	26	10/13	186.9	43.7	179	20.6	35.2	8.3
LB10	155	26	–	–	–	–	–	–	–
Site-mean (G)			8	9.2	−45.3			17.4	13.7
Normal polarity (S)			6			2.3	−16.2	21.9	14.7
Reversal polarity (S)			2			178	9.5	68.2	15
Site-mean (S)			8			0.7	−14.0	28.8	9.8

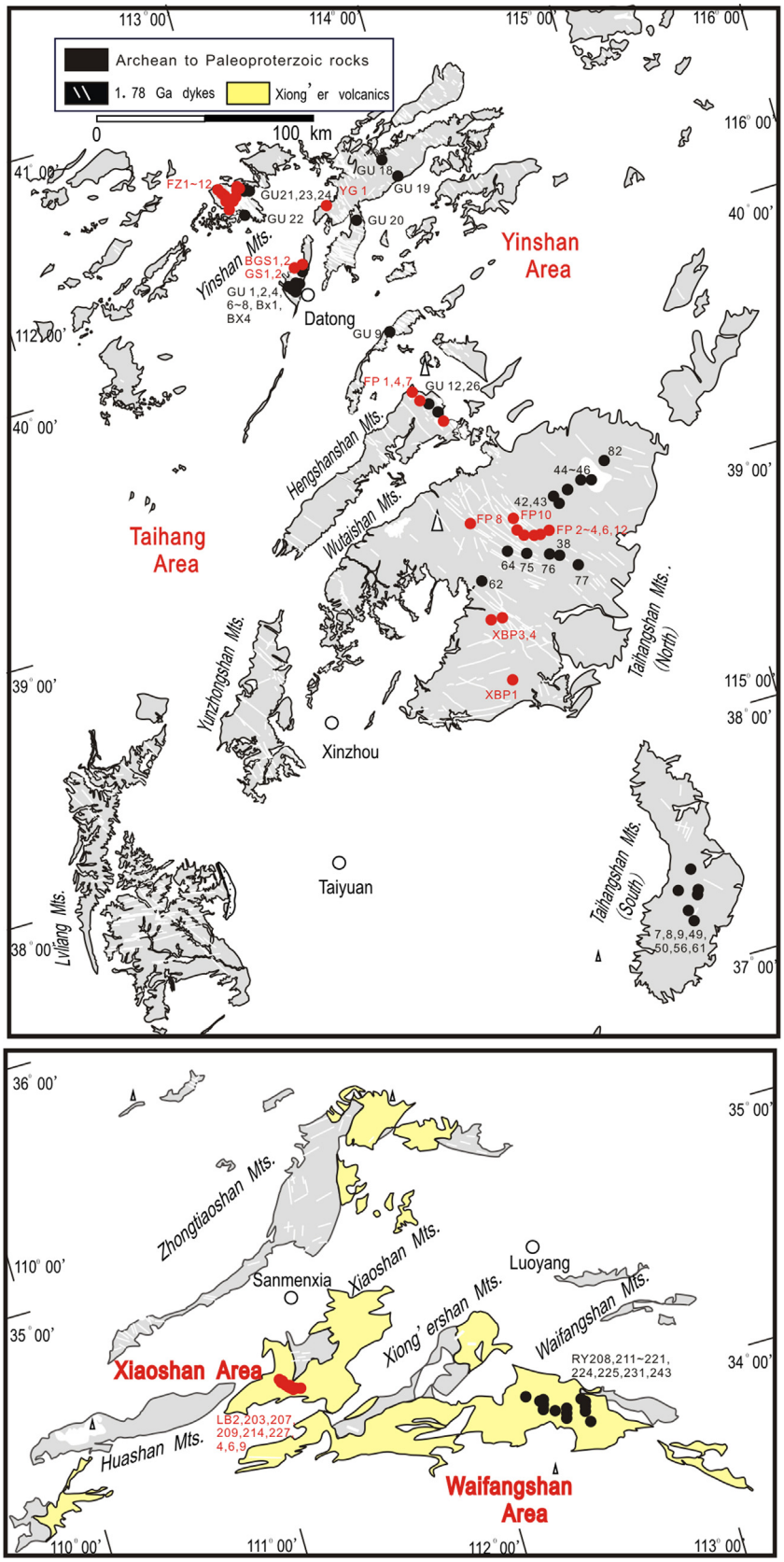

Fig. 12. Distribution of sampling sites of previous studies (black dots) and this study (red dots) in the Yinshan and Taihang areas. Sites named GU** or BX ** are from Halls et al. (2000). Sites numerically named are from Piper et al. (2011). Sites named RY** are from Zhang et al. (2012a). The rest are all from this study. Only the sites which were used to calculate the ~1780 Ma poles in the references are plotted. (For interpretation of reference to color in this figure legend, the reader is referred to the web version of this article.)

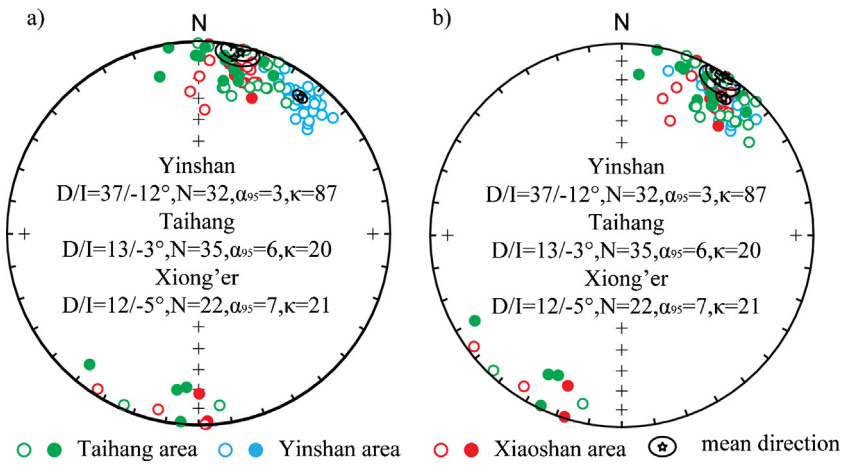

Fig. 13. Equal-area projections of extant site mean directions in the Yinshan (blue), Taihang (green) and Xiong'er areas (red). (a) Compilation of primary results. (b) Compilation of results after rotating (20° clockwise) back the Taihang and Xiong'er areas. All the directions are recalculated to the same reference location (36°N, 112°E). Open (closed) circles in the equal area projections represent downward/upward pointing magnetizations. Open stars with 95 percent confidence circles represent group-mean directions of the samples from different areas. (For interpretation of reference to color in this figure legend, the reader is referred to the web version of this article.)

4.2. Paleo-Mesoproterozoic APWP for NCC

Mesoproterozoic paleomagnetic results were reported from the Jixian section of the NCC (Zhang and Zhang, 1985; Lin, 1988; Zhang et al., 1991; Wu, 2005; Wu et al., 2005; Pei et al., 2005, 2006), although the data generated in the 1980s and 1990s generally were not conducted using modern instruments and data analysis techniques. Due to uncertainties regarding the primary nature of the older studies, we do not consider them further in this analysis. Two paleomagnetic studies of the Yangzhuang Fm. (~1.5 Ga) were carried out in the Jixian sections and indicate a primary magnetization constrained by fold and reversal tests (Pei et al., 2005, 2006; Wu et al., 2005). Considering there were small differences between the results of both studies in the same regions (and stratigraphy), we make a grand average of all the site-mean directions. That exercise yielded a mean direction with $D/I = 83°/+18°$ ($N = 26$ sites, $\kappa = 11$, $\alpha_{95} = 9.1°$). The corresponding paleomagnetic pole is positioned at 12°N, 204°E ($A_{95} = 9°$). Wu (2005) also studied the Mesoproterozoic successions of the Wumishan and Tieling Fms. in Jixian area. The pole with a U-Pb Zircon age (1437 ± 21 Ma, Su et al., 2010) obtained from the Tieling Fm. was located at 12°N, 187°E ($dp/dm = 4.9°/8.1°$) and provides a useful constraint on the position of the NCC at that time. Chen et al. (2013) reported a ~1320 Ma paleomagnetic pole from precisely-dated Mesoproterozoic sills in the NCC (Zhang et al., 2012b). The mean direction of 18 sites after tilt-correction is $D/I = 294°/-32°$ ($\alpha_{95} = 4.3°$), yielding a paleopole at −6° N, 180°E ($A_{95} = 4.3°$).

Combining the previous studies with our new compilation, we sketch a preliminary Paleo-Mesoproterozoic APWP for the NCC (Fig. 15).

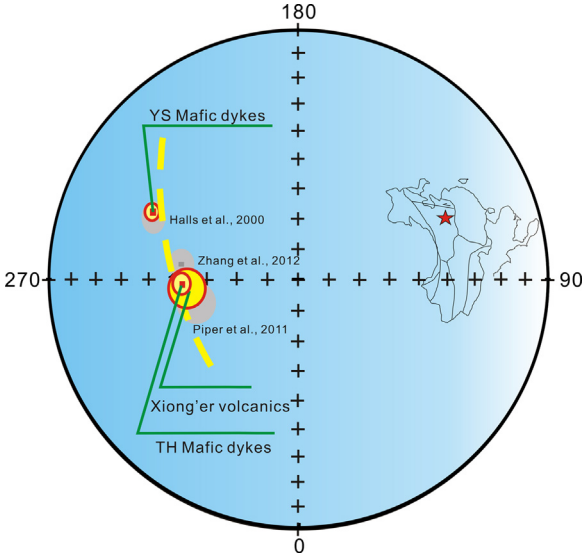

Fig. 14. Equal area plots of paleomagnetic poles of the NCC. The red squares are calculated from combined site-mean results according to the three areas in Fig. 13a. The gray squares with 95 percent confidence circles are the poles reported before. They are distributed along a small circle path centered on the sampling area.

4.3. The paleo-position of the NCC within the Columbia

The paleoposition of the NCC within Columbia is enigmatic. Proposed links of the NCC with the other cratons include Siberia (Li et al., 1996; Halls et al., 2000), India (Piper, 1982; Kröner et al., 1998; Zhao et al., 2002a, 2003; Peng et al., 2005; Hou et al., 2008; Piper et al., 2011), Baltica (Qian, 1997; Wilde et al., 2002; Kusky et al., 2007a; Bispo-Santos et al., 2008), Australia (Zhang et al., 2012a), and Amazonia (Kusky et al., 2007a; Bispo-Santos et al., 2008, 2014). In order to evaluate the various options we selected paleomagnetic data from the aforementioned cratons using the criteria developed by Van der Voo (1990; Table 5).

4.3.1. The relationship between the NCC and the core of Columbia (Laurentia, Baltica and Siberia)

The database from Laurentia is probably the most robust for this time interval. We therefore use Laurentia as the reference point for our discussion. The 1740 Ma pole from Cleaver dykes in western Laurentia was selected as the most reasonable reference comparison to our dykes (Irving et al., 2004). In order to provide a more complete path, we use the following data reference points for Laurentia (see Table 5). For the period ~1.5 Ga, the 1476 Ma St. Francois Mountains igneous province pole was used for comparison with the Yangzhuang Formation of the NCC (Meert and Stuckey, 2002). The slightly younger pole from Tobacco Root Mtns. mafic dykes dated at ca. 1448 Ma (Harlan et al., 2008) is of similar age to the Tieling Fm. A compilation of results from Marcussen and Abrahamsen (1983) and Abrahamsen and Van der Voo (1987) gives a reliable ~1382 Ma pole from the Zig-Zag Dal basalts (Upton et al., 2005). For the younger segment of our analysis we use the pole from the Mackenzie dykes (Buchan and Halls, 1990; Buchan et al., 2000).

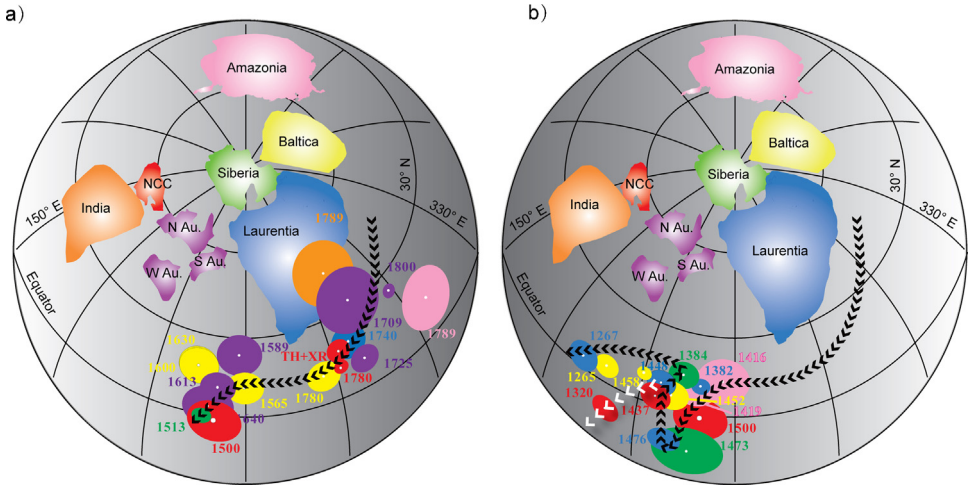

Fig. 15. Selected Paleo-Mesoproterozoic paleomagnetic poles from Laurentia (blue), Baltica (yellow), Siberia (green), Australia (purple), Amazonia (pink), India (light brown) and the NCC (red) and the suggested configuration of Supercontinent Columbia. TH-XR pole is calculated after rotating the results from the Taihang and Xiong'er areas with a 20° clockwise. All paleopoles are rotated to present Laurentia reference frame. The Euler rotation parameters are: Baltica, 47.5°, 1.5°, +49° (Evans and Pisarevsky, 2008); Siberia, 78°, 99°, +147° (Evans and Mitchell, 2011); North Australia, 34.6°, 93.5°, +103.2° (South Australia to North Australia: −18, 134, 51 (Payne et al., 2009); West Australia to North Australia: −20, 135, 40 (Li and Evans, 2011)); Amazonia, 58°, 290.9°, +138°; India, 67°, 103°, 107.6°; the NCC, 45°, 2°, 34°. (For interpretation of reference to color in this figure legend, the reader is referred to the web version of this article.)

For the Baltica segment of the analysis, we use seven poles to evaluate the relationship between the NCC and Baltica. At ~1780 Ma, we use the Q = 7 pole from the Vepsian sandstones of the Shoksha Fm. (Pisarevsky and Sokolov, 2001). Buchan et al. (2000) and Pesonen et al. (2003) averaged two poles around 1630 Ma (~1633 Ma Sipoo quartz porphyry dykes, Mertanen and Pesonen, 1995; ~1628 Ma Sipoo quartz porphyry dykes, Neuvonen, 1986) to yield a mean Baltica pole. Recently, the poles around 1600 Ma for Baltica have been updated with several newly reported poles (Salminen et al., 2014; Klein et al., 2014). We use two poles to

Table 5
Selected paleomagnetic poles from Laurentia, Baltica, Siberia, Australia, Amazonia, India and the NCC.

	Rock type	Age	Plat	Plon	A_{95}	Q	
L1	Cleaver dykes	1740 + 5/−4	19.0	277.0	6.0	6	Irving et al. (2004)
L2	St. Francois mountains	1476 ± 16	−13.0	219.0	7	6	Meert and Stuckey (2002)
L3	Tabacco Root mountain dykes	1448 ± 49	9.0	216.0	10	6	Harlan et al. (2008)
L4	Zig-Zag Dal & intrusions	1382 ± 2	11.0	229.0	3.0	7	Evans and Mitchell (2011), Marcussen and Abrahamsen (1983), Abrahamsen and Van der Voo (1987), Upton et al. (2005)
L5	Mackenzie dykes	1267 ± 2	4.0	190.0	5.0	6	Buchan et al. (2000)
B1	Vepsian sandstones	1790~1770	40.0	221.0	5.0	7	Pisarevsky and Sokolov (2001)
B2	Subjotnian quartz porphyry dykes	1630	29.0	177.0	6.0	6	Buchan et al. (2000)
B3	Satakunta sandstone	1600	28.0	173.0	7	5	Klein et al. (2014)
B4	Satakunta dykes	1565	30.0	192.0	6.0	6	Salminen et al. (2014)
B5	Lake Ladoga mafic rocks	1452 ± 12	15.0	177.0	5.5	6	Lubnina et al. (2010)
B6	Valaam monzodioritic sill	1458 + 4/-3	14.0	166.0	2.4	5	Salminen and Pesonen (2007)
B7	Mean Jotnian intrusions	ca. 1265	4.0	158.0	4.0	6	Buchan et al. (2000)
S1	Fomich River dykes	1513 ± 51	−19.0	78.0	6.0	4	Veselovskiy et al. (2006)
S2	Olenëk mafic intrusions	1473 ± 24	34.0	253.0	10.0	6	Wingate et al. (2009)
S3	Chieress dyke	1384 ± 2	4.0	258.0	9.0	3	Ernst et al. (2000)
N1	Yinshan dykes	1780	35.5	245.2	2.4	6	This study
	TD	1769 ± 2.5	36	247	4.2	6	Halls et al. (2000)
	A1 dykes	~1780	44.1	247.4	15.4	6	Piper et al. (2011)
	A2 dykes	~1780	54.6	283.4	6.5	6	Piper et al. (2011)
	XR	~1780	50.2	263	4.5	6	Zhang et al. (2012a)
	TH-XR	~1780	41.6	246.3	4.3	7	This study
N2	Yangzhuang Fm	1500	11.8	203.9	9.0	7	Wu et al. (2005), Pei et al. (2006)
N3	Tieling Fm	1437 ± 21	12.0	187.0	5.0	7	Wu (2005)
N4	Liaoning, Hebei, sills	1320	−6.0	180.0	4.0	6	Chen et al. (2013)
Au1	Elgee-Pentecost combined	ca. 1800	−5.0	212.0	4.0	5	Schmidt and Williams (2008); Li (2000)
Au2	Peters Creek Vocanics	ca. 1725	−26.0	221.0	5.0	6	Idnurm (2000)
Au3	West Branch Volcanics	1709 ± 3	−16.0	201.0	11.0	6	Idnurm (2000)
Au4	mean Australia	1640	−74.0	183.0	8.0	6	Pesonen et al. (2012)
Au5	Balbirini Dolomite (lower)	1613 ± 4	−66.0	178.0	6.0	5	Idnurm (2000)
Au6	Balbirini Dolomite (upper)	1589 ± 3	−52.0	176.0	8.0	5	Idnurm (2000)
I1	Gwalior traps	1780–1883	15.0	173.0	11.0	4	Pradhan et al. (2010)
I2	Tiruvannamalai	1650 ± 10	−19.0	235.0	9.0	5	Radhakrishna and Joseph (1996)
I3	Lakhna dykes	1466.4 ± 2.6	37.0	133.0	8	5	Pisarevsky et al. (2013)
A1	Avanavero	1788.5 ± 2.5	−48.0	28.0	10	5	Bispo-Santos et al. (2014)
A2	Nova Guarita dykes	1418.5 ± 3.5	−48.0	246.0	7	6	Bispo-Santos et al. (2012)
A3	Indiavaí intrusion	1416	−57.0	250.0	9	4	D'Agrella-Filho et al. (2012)

constrain the position of Baltica around 1450 Ma. These are the ~1452 Ma Lake Ladoga pole (Lubnina et al., 2010) and the 1458 Ma pole from the Valaam monzodioritic sills (Salminen and Pesonen, 2007). The poles are quite similar and the Lake Ladoga pole passes both a baked contact test and a reversal test. The ~1265 Ma was averaged with several earlier results from sills and dykes (Vaasa dolerites pole, Neuvonen, 1966; Market dolerites pole, Neuvonen and Grundström, 1969; Satakunta dolerites pole, Neuvonen, 1965) by both Buchan et al. (2000) and Pesonen et al. (2003) and was frequently used as a key pole.

The situation for establishing the position of Siberia is more problematic. There is no coeval ~1780 Ma pole from Siberia. Veselovskiy et al. (2006) reported a ~1513 Ma (Sm–Nd isochron age) paleomagnetic pole from the igneous rocks in the northern Anabar Uplift. This pole was based on results of 15 dykes/sills with a dual polarity remanence. Although the geochronological age is less precise, we use it as representative of Siberia for that time. The ~1470 Ma pole derived from mafic intrusions in the Kyutingde-Sololi region is precisely dated and has a positive baked contact test (Wingate et al., 2009). The ~1384 Ma Chieress dyke VGP should be reliable and can be used as a potential link to younger poles.

Meert (2014) discusses the limitations of paleomagnetic, geologic and goechronological data in producing Paleo-Mesoproterozoic continental reconstructions. With those caveats in mind, we use the high-quality poles in the discussion above to sketch three APWPs for the Laurentia, Baltica and Siberia (LBS) and note that pole selections can be made such that they all show a similar shape and progression of poles. Due to the fact that we use a similar database, our reconstruction at ~1400 Ma is very similar to that proposed by Evans and Mitchell (2011). By comparing of APWPs between the LBS and the NCC, it is thus noteworthy, that the NCC APWP shows a similar spatial and temporal trend with that of LBS during the ~1800–1450 Ma interval (Fig. 14), implying a close relative paleoposition of the NCC within Columbia. Timing of breakup between the NCC and Columbia is ascertained by the diverging of the APWPs between ~1450 Ma and ~1350 Ma pole, which is similar to the suggestion that the NCC separated from the core of Columbia around 1400 Ma (Zhang et al., 2012a).

4.3.2. The relationship between the NCC and other cratons in Columbia

Many models provide different positions of the NCC within Columbia (e.g. Halls et al., 2000; Zhao et al., 2002a, 2003, 2004; Hou et al., 2008; Peng et al., 2005; Piper et al., 2011; Zhang et al., 2012a; Bispo-Santos et al., 2008, 2012, 2014; D'Agrella-Filho et al., 2012; Chen et al., 2013). However, uncertainties and controversies still exist. Based on the extant geological linkage and paleomagnetic database, we also compiled quality-filtered paleomagnetic poles from other parts of Columbia, e.g. Australia, India and Amazonia, in an effort to establish their relationship with the NCC. Our reconstruction is consistent to Zhang et al.'s (2012) in some way, but with some new findings in the relationship of the NCC with India and Australia.

The ~1780 Ma pole from Kimberley red beds in Australia was reported by Schmidt and Williams (2008). They combined their results with that of Li (2000) to claim a positive fold test. A summary of paleomagnetic poles from Australia was reported by Idnurm (2000). Pesonen et al. (2012) provide a mean 1640 Ma pole for Australia using previously published poles. The 1613 Ma and the 1589 Ma poles from Australia can be placed within the moving trend of the APWP of the core of the Columbia along with the 1725 Ma pole and the 1709 Ma pole. The similar moving trend suggests Australia was part of the supercontinent Columbia during 1780–1500 Ma and positioned to the northwest (present-day coordinates) of Laurentia. Based on polarity/pole choices we can place the North China craton along the present-day margin of northwest Australia during that interval. Geological results indicate that the Jiao-Liao-Ji Orogen was formed after the closure of the rift basin along the southern margin of the NCC at around 1.90–1.85 Ga, and a coeval belt of mafic to intermediate granulite appeared along the southern marigin of the North Australia. Both of these belts are thought to be related to the subduction of Paleoproterozoic oceans (Li et al., 2005; Myers et al., 1996). Our reconstruction implies that the NCC and North Australia may comprise an active continental margin with subduction during the Paleoproterozoic.

Paleomagnetic data from India are relatively fewer in number although several poles have been reported recently. The main problem for our analysis is that the poles that fall into the critical ~1800–1500 Ma intervals are poorly dated. The Gwalior traps pole has a Rb–Sr age of 1789 ± 120 Ma (compiled result cited in Pradhan et al., 2010; Crawford and Compston, 1969). Dykes from the Tiruvannamalai swarm have a poorly defined ^{40}Ar–^{39}Ar age of 1650 ± 10 Ma (Radhakrishna and Joseph, 1996; Radhakrishna et al., 1999). A recent pole was obtained from the Lakhna dykes with a U–Pb zircon age of 1466.4 ± 2.6 Ma (Pisarevsky et al., 2013). Thus, India's APWP is represented by only three poles, of which only one is reliably dated, and comparisons using such poorly dated poles can lead to many erroneous conclusions. If India was part of the Columbia supercontinent, and if Columbia remained a fairly cohesive entity until ~1400 Ma, then, Pisarevsky et al. (2013) used the Lakhna pole to show potential links of India against present-day Laurentia, against Baltica, or adjacent to Siberia. None of the potential fits show good geological correlations so it appears more likely that if India was part of the Columbia supercontinent, it should be placed somewhere other than the options shown in Pisarevsky et al. (2013). It is tempting to compare the ~1790 Ma Gwalior pole with the NCC pole because both blocks share some unique tectonic/geological similarities (Fig. 15a) (Kröner et al., 1998; Zhao et al., 2002a, 2003; Mazumder, 2003; Peng et al., 2005; Hou et al., 2008). Using these two poles, India can be placed along the present-day southern margin of the NCC. The linkage is supported by the provenance of detrital zircons in the NCC and Himalaya and faunal similarities between the NCC and India during the latter part of Neoproterozoic (McKenzie et al., 2011). However, until a reliable age can be established for the Gwalior pole, we caution against making any conclusions regarding India-NCC connections in the Statherian. We also note that a preliminary pole from the NW-SE trending Newer dolerite dykes (1765 Ma; Singhbhum craton, India) may also support the NCC-India connection at ~1780 Ma as it matches the Gwalior pole (ages from Shankar et al., 2014; paleomagnetic data Meert, unpublished).

Amazonia has paleomagnetic data at two periods: 1789 Ma and 1416/1419 Ma (Bispo-Santos et al., 2008, 2012, 2014; D'Agrella-Filho et al., 2012). The 1789 Ma Colider Group pole and the 1789 Ma Avanavero pole were obtained from southern Amazonian Craton and the northern Amazonian Craton, respectively (Bispo-Santos et al., 2008, 2014). The former is regarded as a secondary component or being affected by tectonic movements (Bispo-Santos et al., 2014). With the latter pole and the two 1420 Ma poles—the Nova Guarita dykes pole and the Indiavaí intrusion pole, the reconstruction of Amazonia is broadly consistent with the configuration proposed by Johansson (2009). Some scholars have placed Amazonia next to the present-day southern margin of the NCC and proposed break up during 1789–1420 Ma interval (Bispo-Santos et al., 2008, 2012; D'Agrella-Filho et al., 2012). Unless, and until the database for Amazonia and the NCC are updated with more paleopoles with precise ages, a linkage between Amazonia and the NCC is not testable.

5. Conclusion

A high quality 1780 Ma paleomagnetic pole (245.2°E, 35.5°N, $\kappa = 109.5$, $A_{95} = 2.4°$, N = 32 sites) for the NCC was obtained from a detailed analysis of a large number of the well-dated mafic dykes in the Yinshan Block. By comparing paleomagnetic directions of dykes in different areas, we conclude the dykes in the Taihang area and Xiong'er volcanic rocks might have undergone some local rotation relative to the Yinshan Block and Ordos basin during the Mesozoic-Cenozoic. Due to this rotation, the directions from the Taihang and Xiong'er areas require a rotational correction to establish the proper orientation for the paleomagnetic pole within the NCC. A comparison of our pole (along with previously published Paleo-Mesoproterozoic poles from the NCC) to the available Paleo-Mesoproterozoic paleomagnetic database of Laurentia, Baltica, Siberia, Australia, India and Amazonia yields a variety of possible reconstructions. The reconstructions show some similarities to published models; however all reconstructions suffer from a lack of robust time-space constraints. This is due to the fact that there is often a 100 million year (or more) gap between successive poles. At the same time, the extant data are permissive enough that one could argue that the NCC was part of a larger amalgam of continents during the 1800–1450 Ma intervals. We provide reconstructions as a means to examine possible relationships between the NCC and other blocks and show that a position of the NCC adjacent to the present-day NW Australian margin during 1780–1500 Ma intervals is worthy of further testing.

Acknowledgements

This work was supported by the National Natural Science Foundation of China (Grant Nos. 90814000, 90814002) and the USA National Science Foundation grant EAR09-10888 (to JGM). We greatly appreciate discussions with and help from Sheng Huang, Kunpeng Ge, Chengying Liu, Lu Su, Bailing Wu, Yanfen Kong, Suzhen Liu. An anonymous reviewer and Dr. D. Evans, guest Editor Dr. S.A. Pisarevsky and Editor Dr. G. Zhao are appreciated for very useful suggestions that improve greatly our paper.

References

Abrahamsen, N., Van der Voo, R., 1987. Paleomagnetism of middle Proterozoic (c. 1.25 Ga) dykes from central North Greenland. Geophys. J. R. Astronom. Soc. 91, 597–611.

Berthelsen, A., Marker, M., 1986. Tectonics of the Kola collision suture and adjacent Archean and Early Proterozoic terrains in the northeastern region of the Baltic Shield. Tectonophysics 126, 31–55.

Biggin, A.J., van Hinsbergen, D.J.J., Langereis, C.G., Straathof, G.B., Deenen, M.H.L., 2008. Geomagnetic secular variation in the Cretaceous Normal Superchron and in the Jurassic. Phys. Earth Planet. Inter. 169, 3–19.

Bispo-Santos, F., D'Agrella-Filho, M.S., Pacca, I.I.G., Janikian, L., Trindade, R.I.F., Elming, S.Å., Silva, J.A., Barros, M.A.S., Pinho, F.E.C., 2008. Columbia revisited: paleomagnetic results from the 1790Ma Colider volcanics (SW Amazonian Craton, Brazil). Precambrian Res. 164, 40–49.

Bispo-Santos, F., D'Agrella-Filho, M.S., Trindade, R.I., Elming, S.Å., Janikian, L., Vasconcelos, P.M., Perillo, B.M., Pacca, I.I.G., Silva, J.A., Barros, M.A.S., 2012. Tectonic implications of the 1419Ma Nova Guarita mafic intrusives paleomagnetic pole (Amazonian Craton) on the longevity of Nuna. Precambrian Res. 196, 1–22.

Bispo-Santos, F., D'Agrella-Filho, M.S., Trindade, R.I., Janikian, L., Reis, N.J., 2014. Was there SAMBA in Columbia? Paleomagnetic evidence from 1790Ma Avanavero mafic sills (northern Amazonian Craton). Precambrian Res. 244, 139–155.

Buchan, K., Halls, H., 1990. Paleomagnetism of Proterozoic mafic dyke swarms of the Canadian Shield. In: Mafic Dykes and Emplacement mechanisms. Balkema, Rotterdam, pp. 209–230.

Buchan, K., Mertanen, S., Park, R., Pesonen, L., Elming, S.Å., Abrahamsen, N., Bylund, G., 2000. Comparing the drift of Laurentia and Baltica in the Proterozoic: the importance of key paleomagnetic poles. Tectonophysics 319, 167–198.

Chen, L.-W., Huang, B.-C., Yi, Z.-Y., Zhao, J., Yan, Y.-G., 2013. Paleomagnetism of ca. 1.35Ga sills in northern North China Craton and implications for paleogeographic reconstruction of the Mesoproterozoic supercontinent. Precambrian Res. 228, 36–47.

Condie, K.C., 2002. Breakup of a Paleoproterozoic supercontinent. Gondwana Res. 5, 41–43.

Crawford, A.R., Compston, W., 1969. The age of the Vindhyan System of Peninsular India. Quater. J. Geol. Soc. Lond. 125, 351–371.

Cui, M.-L., Zhang, B.-L., Peng, P., Zhang, L.-C., Shen, X.-L., Guo, Z.-H., Huang, X.-F., 2010. Zircon/baddeleyite U–Pb dating for the Paleo-proterozoic intermediate-acid intrusive rocks in Xiaoshan Mountains, west of Henan Province and their constraints on the age of the Xiong'er Volcanic Province. Acta Petrol. Sin. 26 (5), 1541–1549.

D'Agrella-Filho, M.S., Trindade, R.I.F., Elming, S.Å., Teixeira, W., Yokoyama, E., Tohver, E., Geraldes, M.C., Pacca, I.I.G., Barros, M.A.S., Ruiz, A.S., 2012. The 1420 Ma Indiavaí Mafic Intrusion (SW Amazonian Craton): Paleomagnetic results and implications for the Columbia supercontinent. Gondwana Res. 22, 956–973.

Deng, Q.-D., Zhang, P.-Z., 2002. Characteristics of active tectonics in China. Sci. China Ser. D: Earth Sci. 32, 1020–1030.

Dunlop, D.J., 2002a. Theory and application of the Day plot (Mrs/Ms versus Hcr/Hc) 1. Theoretical curves and tests using titanomagnetite data. J. Geophys. Res.: Solid Earth (1978–2012) 107 (EPM 4-1-EPM 4-22).

Dunlop, D.J., 2002b. Theory and application of the Day plot (Mrs/Ms versus Hcr/Hc) 1. Theoretical curves and tests using titanomagnetite data. J. Geophys. Res.: Solid Earth (1978–2012) 107 (EPM 5-1-EPM 5-15).

Ernst, R., Buchan, K., Hamilton, M., Okrugin, A., Tomshin, M., 2000. Integrated paleomagnetism and U–Pb geochronology of mafic dikes of the Eastern Anabar Shield Region, Siberia: implications for Mesoproterozoic Paleolatitude of Siberia and comparison with laurentia. J. Geol. 108, 381–401.

Evans, D.A.D., Pisarevsky, S.A., 2008. Plate tectonics on early Earth? Weighing the paleomagnetic evidence. In: Condie, K.C., Pease, V. (Eds.), When Did Plate Tectonics Begin on Planet Earth? Geological Society of America Special Papers, pp. 249–263.

Evans, D.A.D., Mitchell, R.N., 2011. Assembly and breakup of the core of Paleoproterozoic–Mesoproterozoic supercontinent Nuna. Geology 39, 443–446.

Fisher, R., 1953. Dispersion on a sphere. Proc. R. Soc. Lond. Ser. A. Math. Phys. Sci. 217, 295–305.

Guo, J.-H., Sun, M., Chen, F.-K., Zhai, M.-G., 2005. Sm–Nd and SHRIMP U–Pb zircon geochronology of high-pressure granulites in the Sanggan area, North China Craton: timing of Paleoproterozoic continental collision. J. Asian Earth Sci. 24, 629–642.

Halls, H.C., Li, J.-H., Davis, D., Hou, G.-T., Zhang, B.-X., Qian, X.-L., 2000. A precisely dated Proterozoic paleomagnetic pole from the North China craton, and its relevance to paleocontinental reconstruction. Geophys. J. Int. 143, 185–203.

Harlan, S.S., Geissman, J.W., Snee, L.W., 2008. Paleomagnetism of Proterozoic mafic dikes from the Tobacco Root Mountains, southwest Montana. Precambrian Res. 163, 239–264.

HBGMR, (Hebei Bureau of Geology and Mineral Resources), 1982. Regional Geology of Hebei Province, Beijing Municipality and Tianjin Municipality. Geological Publishing House, Beijing, pp. 1–741 (in Chinese with English abstract).

He, Y.-H., Zhao, G.-C., Sun, M., Xia, X.-P., 2009. SHRIMP and LA-ICP-MS zircon geochronology of the Xiong'er volcanic rocks: implications for the Paleo-Mesoproterozoic evolution of the southern margin of the North China Craton. Precambrian Res. 168, 213–222.

Huang, B.-C., Shi, R.-P., Wang, Y.-C., Zhu, R.-X., 2005. Palaeomagnetic investigation on Early–Middle Triassic sediments of the North China block: a new Early Triassic palaeopole and its tectonic implications. Geophys. J. Int. 160, 101–113.

Hou, G.-T., Li, J.-H., Qian, X.-L., Zhang, B.-X., Halls, H.C., 2001. The paleomagnetism and geological significance of Mesoproterozoic dyke swarms in the central North China craton. Sci. China Ser. D: Earth Sci. 44 (2), 185–192.

Hou, G.-T., Santosh, M., Qian, X.-L., Lister, G.S., Li, J.-H., 2008. Configuration of the Late Paleoproterozoic supercontinent Columbia: Insights from radiating mafic dyke swarms. Gondwana Res. 14, 395–409.

Idnurm, M., 2000. Towards a high resolution Late Paleoproterozoic–earliest Mesoproterozoic apparent polar wander path for northern Australia. Aust. J. Earth Sci. 47, 405–429.

Irving, E., Baker, J., Hamilton, M., Wynne, P.J., 2004. Early Proterozoic geomagnetic field in western Laurentia: implications for paleolatitudes, local rotations and stratigraphy. Precambrian Res. 129, 251–270.

Johansson, Å., 2009. Baltica, Amazonia and the SAMBA connection—1000 million years of neighborhood during the Proterozoic? Precambrian Res. 175, 221–234.

Kirschvink, J., 1980. The least-squares line and plane and the analysis of paleomagnetic data. Geophys. J. Int. 62, 699–718.

Klein, R., Pesonen, L., Salminen, J., Mertanen, S., 2014. Paleomagnetism of Mesoproterozoic Satakunta sandstone, Western Finland. Precambrian Res. 244, 156–169.

Kröner, A., Cui, W.-Y., Wang, S.-Q., Wang, C.-Q., Nemchin, A.A., 1998. Single zircon ages from high-grade rocks of the Jianping Complex, Liaoning Province, NE China. J. Asian Earth Sci. 16, 519–532.

Kröner, A., Wilde, S.A., Li, J.-H., Wang, K.-Y., 2005. Age and evolution of a late Archean to Paleoproterozoic upper to lower crustal section in the Wutaishan/Hengshan/Fuping terrain of northern China. J. Asian Earth Sci. 24, 577–595.

Kusky, T.M., Li, J.-H., 2003. Paleoproterozoic tectonic evolution of the North China Craton. J. Asian Earth Sci. 22, 383–397.

Kusky, T.M., Li, J.-H., Santosh, M., 2007a. The Paleoproterozoic north Hebei orogen: North China Craton's collisional suture with the Columbia supercontinent. Gondwana Res. 12, 4–28.

Kusky, T.M., Windley, B.F., Zhai, M.-G., 2007b. Tectonic evolution of the North China Block: from orogen to craton to orogen. Geol. Soc. London Special Publications 280, 1–34.

Li, J.-H., Qian, X.-L., Huang, X.-N., Liu, S.-W., 2000. Tectonic framework of North China Block and its cratonization in the early Precambrian. Acta Petrol. Sin. 16 (1), 1–10.

Li, J.-H., Hou, G.-T., Qian, X.-L., Halls, H.C., Don, D., 2001. Single zircon U–Pb age of the initial Mesoproterozoic basic dyke swarms in Hengshan Mountain and its implication for the tectonic evolution of the North China Craton. Geol. Rev. 47 (3), 234–238.
Li, S.-Z., Zhao, G.-C., Sun, M., Han, Z.-Z., Luo, Y., Hao, D.-F., Xia, X.-P., 2005. Deformation history of the Paleoproterozoic Liaohe assemblage in the Eastern Block of the North China Craton. J. Asian Earth Sci. 24, 659–674.
Li, T.-S., Zhai, M.-G., Peng, P., Chen, L.-A., Guo, J.-H., 2010. Ca. 2.5 billion year old coeval ultramafic-mafic and syenitic dykes in Eastern Hebei: Implications for cratonization of the North China Craton. Precambrian Res. 180, 143–155.
Li, Z.-X., 2000. Paleomagnetic evidence for unification of the North and West Australian cratons by ca. 1.7 Ga: new results from the Kimberley Basin of northwestern Australia. Geophys. J. Int. 142, 173–180.
Li, Z.-X., Zhang, L., Powell, C.M., 1996. Positions of the East Asian cratons in the Neoproterozoic supercontinent Rodinia. Aust. J. Earth Sci. 43, 593–604.
Li, Z.-X., Evans, D.A.D., 2011. Late Neoproterozoic 40° intraplate rotation within Australia allows for a tighter-fitting and longer-lasting Rodinia. Geology 39 (1), 39–42.
Lin, J.-L., 1988. Middle to Late Proterozoic paleomagnetic results from Jixian. Chin. Sci. Bull. 33, 207–210.
Lubnina, N.V., Mertanen, S., Söderlund, U., Bogdanova, S., Vasilieva, T.I., Frank-Kamenetsky, D., 2010. A new key pole for the East European Craton at 1452 Ma: Paleomagnetic and geochronological constraints from mafic rocks in the Lake Ladoga region (Russian Karelia). Precambrian Res. 183, 442–462.
McFadden, P., 1990. A new fold test for palaeomagnetic studies. Geophys. J. Int. 103, 163–169.
Marcussen, C., Abrahamsen, N., 1983. Paleomagnetism of the Proterozoic Zig-Zag Dal Basalt and the Midsommersø Dolerites, eastern North Greenland. Geophys. J. R. Astron. Soc. 73, 367–387.
Mazumder, R., 2003. Correlations between the Eastern Block of the North China craton and the South Indian Block of the Indian Shield: an Archean to Paleoproterozoic link. Precambrian Res. 127, 379–380.
Meert, J.G., Stuckey, W., 2002. Revisiting the paleomagnetism of the 1.476 Ga St. Francois Mountains igneous province, Missouri. Tectonics 21, 1007.
Meert, J.G., 2002. Paleomagnetic evidence for a Paleo-Mesoproterozoic supercontinent Columbia. Gondwana Res. 5 (1), 207–215.
Meert, J.G., 2014. Strange attractors, spiritual interlopers and lonely wanderers: The search for pre-Pangean supercontinents. Geosci. Front. 5, 155–166.
Meng, Q.-R., Zhang, G.-W., 1999. Timing of collision of the North and South China blocks: controversy and reconciliation. Geology 27, 123–126.
Mertanen, S., Pesonen, L.J., 1995. Palaeomagnetic and rock magnetic investigations of the Sipoo Subjotnian quartz porphyry and diabase dykes, southern Fennoscandia. Phys. Earth Planet. Interiors 88 (3), 145–175.
Myers, J.S., Shaw, R.D., Tyler, I.M., 1996. Tectonic evolution of Proterozoic Australia. Tectonics 15, 1431–1446.
Neuvonen, K.J., 1965. Palaeomagnetism of the dike systems in Finland: I. Remanent magnetization of Jotnian olivine dolerites in southwestern Finland. Bul. Geol. Soc. Finl. 37, 153–168.
Neuvonen, K.J., 1966. Palaeomagnetism of the dike systems in Finland, II, remanent magnetization of dolerites in the Vaasa archipelago. Bull. Geol. Soc. Finl. 38, 275–281.
Neuvonen, K.J., Grundström, L., 1969. Palaeomagnetism of the dike systems in Finland, IV, remanent magnetization of the dolerite and related dikes in the Aland archipelago. Bull. Geol. Soc. Finl. 41, 57–63.
Neuvonen, K.J., 1986. On the direction of remanent magnetization of the quartz porphyry dikes in SE Finland. Bull. Geol. Soc. Finl. 58 (1), 195–201.
Payne, J.L., Hand, M., Barovich, K.M., Reid, A., Evans, D.A.D., 2009. Correlations and reconstruction models for the 2500–1500 Ma evolution of the Mawson Continent. Geol. Soc. London; Special Publications 323 (1), 319–355.
Pei, J.-L., Yang, Z.-Y., Zhao, Y., 2005. New Mesoproterozoic paleomagnetic results in North China and its implication for the Columbia supercontinent. Geol. Bull. China 24 (6), 496–498.
Pei, J.-L., Yang, Z.-Y., Zhao, Y., 2006. A Mesoproterozoic paleomagnetic pole from the Yangzhuang Formation, North China and its tectonics implications. Precambrian Res. 151, 1–13.
Peng, P., Zhai, M.-G., Zhang, H.-F., Guo, J.-H., 2005. Geochronological constraints on the Paleoproterozoic evolution of the North China craton: SHRIMP zircon ages of different types of Mafic dikes. Int. Geol. Rev. 47, 492–508.
Peng, P., Zhai, M.-G., Guo, J.-H., 2006. 1.80–1.75 Ga mafic dyke swarms in the central North China craton: implications for a plume-related break-up event. In: Hanski, E., Mertanen, S., Ramö, T., Vuollo, J. (Eds.), Dyke Swarms—Time Markers of Crustal Evolution. A.A. Balkema Publishers.
Peng, P., Zhai, M.-G., Ernst, R.E., Guo, J.-H., Liu, F., Hu, B., 2008. A 1.78 Ga large igneous province in the North China craton: The Xiong'er volcanic province and the North China dyke Swarm. Lithos 101, 260–280.
Peng, P., 2010. Reconstruction and interpretation of giant mafic dyke swarms: a case study of 1.78 Ga magmatism in the North China craton. Geol. Soc. London, Special Publications 338, 163–178.
Peng, P., 2014. Precambrian mafic dyke swarms in the North China Craton and their potential geological implications. Sci. China-Earth Sci. (in press).
Pesonen, L.J., Elming, S.Å., Mertanen, S., Pisarevsky, S., D'Agrella-Filho, M.S., Meert, J.G., Schmidt, P.W., Abrahamsen, N., Bylund, G., 2003. Paleomagnetic configuration of continents during the Proterozoic. Tectonophysics 375, 289–324.
Pesonen, L.J., Mertanen, S., Veikkolainen, T., 2012. Paleo-Mesoproterozoic supercontinents – a paleomagnetic view. Geophysica 48, 5–47.
Piper, J.D.A., 1982. The Precambrian paleomagnetic record: the case for the Proterozoic Supercontinent. Earth Planet Sci. Lett. 59, 61–89.
Piper, J.D.A., Zhang, J.-S., Huang, B.-C., Roberts, A.P., 2011. Paleomagnetism of Precambrian Dyke Swarms in the North China Shield: The 1.8 Ga LIP event and crustal consolidation in late Paleoproterozoic times. J. Asian Earth Sci. 41, 504–524.
Pisarevsky, S.A., Sokolov, S.J., 2001. The magnetostratigraphy and a 1780 Ma paleomagnetic pole from the red sandstones of the Vazhinka River section, Karelia, Russia. Geophys. J. Int. 146, 531–538.
Pisarevsky, S.A., Biswal, T.K., Wang, X.-C., De Waele, B., Ernst, R., Söderlund, U., Tait, J.A., Ratre, K., Singh, Y.K., Cleve, M., 2013. Palaeomagnetic, geochronological and geochemical study of Mesoproterozoic Lakhna Dykes in the Bastar Craton, India: implications for the Mesoproterozoic supercontinent. Lithos 174, 125–143.
Pradhan, V.R., Meert, J.G., Pandit, M.K., Kamenov, G., Gregory, L.C., Malone, S.J., 2010. India's changing place in global Proterozoic reconstructions: a review of geochronologic constraints and paleomagnetic poles from the Dharwar, Bundelkhand and Marwar cratons. J. Geodyn. 50, 224–242.
Qian, X.-L., Chen, Y.-P., 1987. Late Precambrian mafic dyke swarms of the North China craton. Mafic Dyke Swarms. Geol. Assoc. Can. Special Papers 34, 385–391.
Qian, X.-L., 1997. Tectonic correlations of the precambrian evolution of the North China craton with the baltic shield. Precambrian Geology and Metamorphic Petrology, Utrcht, the Netherlands, pp. 43–58.
Radhakrishna, T., Joseph, M., 1996. Proterozoic paleomagnetism of the mafic dyke swarms in the high-grade region of southern India. Precambrian Res. 76, 31–46.
Radhakrishna, T., Maluski, H., Mitchell, J., Joseph, M., 1999. $^{40}Ar/^{39}Ar$ and K/Ar geochronology of the dykes from the South Indian granulite terrain. Tectonophysics 304, 109–129.
Roberts, A.P., Cui, Y.-L., Verosub, K.L., 1995. Wasp-waisted hysteresis loops: mineral magnetic characteristics and discrimination of components in mixed magnetic systems. J. Geophys. Res. 100, 17909–17924.
Rogers, J.J.W., 1996. A history of continents in the past three billion years. J. Geol. 104, 91–107.
Rogers, J.J.W., Santosh, M., 2002. Configuration of Columbia, a Mesoproterozoic supercontinent. Gondwana Res. 5, 5–22.
Salminen, J., Pesonen, L.J., 2007. Paleomagnetic and rock magnetic study of the Mesoproterozoic sill, Valaam island, Russian Karelia. Precambrian Res. 159, 212–230.
Salminen, J., Mertanen, S., Evans, D., Wang, Z., 2014. Paleomagnetic and geochemical studies of the Mesoproterozoic Satakunta dyke swarms, Finland, with implications for a Northern Europe–North America (NENA) connection within Nuna supercontinent. Precambrian Res. 244, 170–191.
Schmidt, P.W., Williams, G.E., 2008. Paleomagnetism of red beds from the Kimberley Group, Western Australia: Implications for the paleogeography of the 1.8 Ga King Leopold glaciation. Precambrian Res. 167, 267–280.
Shankar, R., Vijayagopal, B., Kumar, A., 2014. Precise Pb–Pb baddeleyite ages of 1765 Ma for a Singhbhum 'newer dolerite' dyke swarm. Curr. Sci. 106, 1306–1310.
Shi, R.-P., Huang, B.-C., Zhu, R.-X., Ren, S.-M., 2004. Palaeomagnetic study of Early Triassic red beds from Jiaocheng, Shanxi Province: Local rotation and tectonic significance. Sci. China Ser. D: Earth Sci. 47, 108–114.
Su, W.-B., Zhang, S.-H., Huff, W.D., Li, H.-K., Ettensohn, F.R., Chen, X.-Y., Yang, H.-M., Han, Y.-G., Song, B., Santosh, M., 2010. SHRIMP U-Pb dating for a K-bentonite bed in the Tieling Formation, North China. Chin. Sci. Bull. 55, 3312–3323.
Uno, K., Huang, B.-C., 2003. Constraints on the Jurassic swing of the apparent polar wander path for the North China Block. Geophys. J. Int. 154, 801–810.
Upton, B.G.J., Rämö, O.T., Heaman, L.M., Blichert-Toft, J., Kalsbeek, F., Barry, T.L., Jepsen, H.F., 2005. The Mesoproterozoic Zig-Zag Dal basalts and associated intrusions of eastern North Greenland: mantle plume–lithosphere interaction. Contrib. Mineral. Petrol. 149, 40–56.
Van der Voo, R., 1990. The reliability of paleomagnetic data. Tectonophysics 184, 1–9.
Veselovskiy, R.V., Petrov, P.Y., Karpenko, S.F., Kostitsyn, Y.A., Pavlov, V.E., 2006. New Paleomagnetic and isotopic data on the Mesoproterozoic igneous complex on the northern slope of the Anabar uplift. Doklady Earth Sci. 411 (8), 1190–1194.
Wang, X.-L., Jiang, S.-Y., Bai, B.-Z., 2010. Melting of enriched Archean subcontinental lithospheric mantle: Evidence from the ca. 1760 Ma volcanic rocks of the Xiong'er Group, southern margin of the North China Craton. Precambrian Res. 182, 204–216.
Wang, Y.-J., Fan, W.-M., Zhang, Y.-H., Guo, F., Zhang, H.-F., Peng, T.-P., 2004. Geochemical, $^{40}Ar/^{39}Ar$ geochronological and Sr–Nd isotopic constraints on the origin of Paleoproterozoic mafic dikes from the southern Taihang Mountains and implications for the ca. 1800 Ma event of the North China Craton. Precambrian Res. 135, 55–77.
Wilde, S.A., Zhao, G.-C., Sun, M., 2002. Development of the North China Craton during the late Archean and its final amalgamation at 1.8 Ga: some speculations on its position within a global Paleoproterozoic supercontinent. Gondwana Res. 5, 85–94.
Wingate, M.T.D., Pisarevsky, S.A., Gladkochub, D.P., Donskaya, T.V., Konstantinov, K.M., Mazukabzov, A.M., Stanevich, A.M., 2009. Geochronology and paleomagnetism of mafic igneous rocks in the Olenek Uplift, northern Siberia: implications for Mesoproterozoic supercontinents and paleogeography. Precambrian Res. 170, 256–266.
Wu, C.-H., Li, H.-M., Zhong, C.-T., Chen, Q.-A., 1998. The ages of zircon and rutile(cooling) from Khondalite in Huangtuyao, Inner Mongolia. Geol. Rev. 44, 618–626.
Wu, C.-H., Zhong, C.-T., 1998. Early Proterozoic SW-NE collision model for the central part of the North China Craton: implications for tectonic regime of the khondalite

downward into lower crust in Jin-Meng high-grade region. Progr. Precambrian Res. 21, 28–50.
Wu, H.-C., (Doctoral paper) 2005. New paleomagnetic results from Mesoproterozoic successions in Jixian area, North China Block, and their implications for paleocontinental reconstructions. Chinese University of Geoscience, Beijing, pp. 1–133.
Wu, H.-C., Zhang, S.-H., Li, Z.-X., Li, H.-Y., Dong, J., 2005. New paleomagnetic results from the Yangzhuang Formation of the Jixian System, North China, and tectonic implications. Chin. Sci. Bull. 50, 1483–1489.
Yang, Z.-Y., Besse, J., 2001. New Mesozoic apparent polar wander path for south China: tectonic consequences. J. Geophys. Res.: Solid Earth (1978–2012) 106, 8493–8520.
Yang, Z.-Y., Courtillot, V., Besse, J., Ma, X.-H., Xing, L.-S., Xu, S.-J., Zhang, J.-X., 1992. Jurassic paleomagnetic constraints on the collision of the North and South China blocks. Geophys. Res. Lett. 19, 577–580.
Yuan, W., Yang, Z.-Y., 2014. The Alashan Terrane did not amalgamate with North China block by the Late Permian: Evidence from Carboniferous and Permian paleomagnetic results. J. Asian Earth Sci., http://dx.doi.org/10.1016/j.jseaes.2014.02.010.
Zhai, M.-G., Bian, A.-G., Zhao, T.-P., 2000. The amalgamation of the supercontinent of North China Craton at the end of Neo-Archaean and its breakup during late Paleoproterozoic and Mesoproterozoic. Sci. China Ser. D: Earth Sci. 43, 219–232.
Zhai, M.-G., Liu, W.-J., 2003. Paleoproterozoic tectonic history of the North China craton: a review. Precambrian Res. 122, 183–199.
Zhai, M.-G., Peng, P., 2007. Paleoproterozoic events in the north China craton. Acta Petrol. Sin. 23, 2665–2682.
Zhang, H.-M., Zhang, W.-Z., 1985. Paleomagnetic data, late Precambrian magnetostratigraphy and tectonic evolution of eastern China. Precambrian Res. 29, 65–75.
Zhang, H.-M., Zhang, W.-Z., Elston, D.P., 1991. Paleomagnetic study on Middle and Late Proterozoic rock in Jixian, North China. Acta Geophys. Sin. 34, 602–615.
Zhang, S.-H., Li, Z.-X., Evans, D.A.D., Wu, H.-C., Li, H.-Y., Dong, J., 2012a. Pre-Rodinia supercontinent Nuna shaping up: A global synthesis with new paleomagnetic results from North China. Earth Planet. Sci. Lett. 353, 145–155.
Zhang, S.-H., Zhao, Y., Santosh, M., 2012b. Mid-Mesoproterozoic bimodal magmatic rocks in the northern North China Craton: implications for magmatism related to breakup of the Columbia supercontinent. Precambrian Res. 222, 339–367.
Zhang, Y.-Q., Ma, Y.-S., Nong, Y., Wei, S., Dong, S.-W., 2003. Cenozoic extensional stress evolution in North China. J. Geodyn. 36, 591–613.
Zhao, G.-C., Wilde, S.A., Cawood, P.A., Sun, M., 2001. Archean blocks and their boundaries in the North China. Craton: lithological, geochemical, structural and PT path constraints and tectonic evolution. Precambrian Res. 107, 45–73.
Zhao, G.-C., Cawood, P.A., Wilde, S.A., Sun, M., 2002a. Review of global 2.1–1.8 Ga orogens: implications for a pre-Rodinia supercontinent. Earth-Sci. Rev. 59, 125–162.
Zhao, T.-P., Zhou, M.-F., Zhai, M.-G., Xia, B., 2002b. Paleoproterozoic rift-related volcanism of the Xiong'er Group, North China Craton: implications for the breakup of Columbia. Int. Geol. Rev. 44, 336–351.
Zhao, G.-C., Sun, M., Wilde, S.A., 2003. Correlations between the eastern block of the North China craton and the south Indian block of the Indian Shield: an Archaean to Paleoproterozoic link. Precambrian Res. 122, 201–233.
Zhao, G.-C., Sun, M., Wilde, S.A., Li, S.-Z., 2004. A Paleo-Mesoproterozoic supercontinent: assembly, growth and breakup. Earth-Sci. Rev. 67, 91–123.
Zhao, G.-C., Sun, M., Wilde, S.A., Li, S.-Z., 2005. Late Archean to Paleoproterozoic evolution of the North China Craton: key issues revisited. Precambrian Res. 136, 177–202.
Zhao, X.-X., Coe, R., Wu, H.-N., Zhao, Z.-Y., 1993. Silurian and Devonian paleomagnetic poles from North China and implications for Gondwana. Earth Planet. Sci. Lett. 117, 497–506.
Zijderveld, J., 1967. AC demagnetization of rocks: analysis of results. Methods Paleomag., 254–286.